



**The btp [2,6-bis(1,2,3-triazol-4-yl)pyridine] binding motif:
A new versatile terdentate ligand for applications in
coordination, supramolecular and material chemistry**

Journal:	<i>Chemical Society Reviews</i>
Manuscript ID:	CS-REV-03-2014-000120.R1
Article Type:	Review Article
Date Submitted by the Author:	10-May-2014
Complete List of Authors:	Gunnlaugsson, Thorfinnur; Trinity College Dublin, School of Chemistry Byrne, Joseph; Trinity College Dublin, Chemistry Kitchen, Jonathan; University of Southampton, Chemistry

Cite this: DOI: 10.1039/c0xx00000x

www.rsc.org/xxxxxx

ARTICLE TYPE

The **btp** [2,6-bis(1,2,3-triazol-4-yl)pyridine] binding motif: A new versatile terdentate ligand for supramolecular and coordination chemistry

Joseph P. Byrne,^{*a} Jonathan A. Kitchen^b and Thorfinnur Gunnlaugsson^{*a}

⁵ Received (in XXX, XXX) Xth XXXXXXXXX 20XX, Accepted Xth XXXXXXXXX 20XX
DOI: 10.1039/b000000x

Ligands containing the **btp** [2,6-bis(1,2,3-triazol-4-yl)pyridine] motif have appeared with increasing regularity over the last decade. This class of ligands, formed in a one pot ‘click’ reaction has been studied for various purposes, such as for generating d and f metal coordination complexes and supramolecular self-assemblies, and in the formation of dendritic and polymeric networks, *etc.* This review article introduces **btp** as a novel and highly versatile terdentate building block with huge potential in inorganic supramolecular chemistry. We will focus on the coordination chemistry of **btp** ligands with a wide range of metals, and how it compares with other classical pyridyl and polypyridyl based ligands, and then present a selection of applications including use in catalysis, enzyme inhibition, photochemistry, molecular logic and materials, *e.g.* polymers, dendrimers and gels. The photovoltaic potential of triazolium derivatives of **btp** and its interactions with anions will also be discussed.

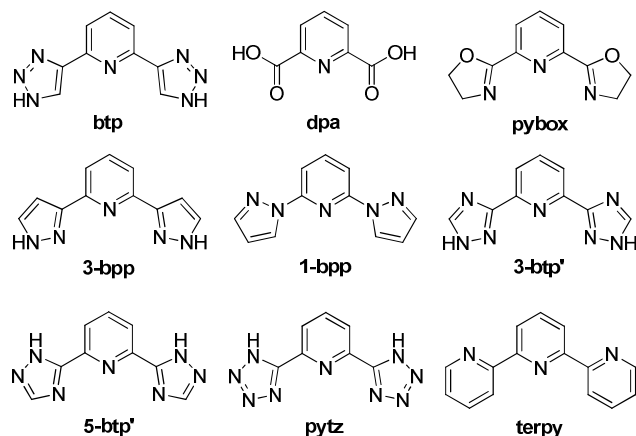
1. Introduction

The objective of this review is to give a comprehensive overview of the chemistry of the **btp** motif [2,6-bis(1,2,3-triazol-4-yl)pyridine], Scheme 1, which is chiefly employed as a terdentate ligand, but which also displays interactions with anions and has been demonstrated to act as a C^N^C chelate upon alkylation. Given the range of fields and the potentially wide-ranging applications that this versatile class of ligand has to offer, there has been a surprising paucity of publications reporting the synthesis of such ligands and complexes to date. To the best of our knowledge, between 2004 and 2014, only 55 articles have been published that focus on the use of **btp**-based systems, with nearly a third of those examples published since 2013. There is vast potential in the study of these systems, which has grown significantly in recent years and will certainly continue apace. Hence, given our own interest in this building block, and the fact that its application will certainly grow steadily in the years to come, we felt it was timely to review this new and exciting class of ligand.

1.1 Terdentate ligands

Terdentate pyridine-centred heteroaromatic ligands represent particularly privileged coordination frameworks that are used in a wide range of research fields, such as in coordination chemistry and supramolecular self-assembly, in photochemical and optoelectronic applications and in the developments of catalysts and magnetic materials. A variety of terdentate coordinating motifs have been reported in the literature to date; including (but not limited to) derivatives of dipicolinic acid (**dpa**), 2,6-bis(oxazoline)-pyridine (**pybox**), 2,6-di(pyrazolyl)pyridines

(**bpp**), bis(1,2,4-triazolyl)pyridines (**btp'**), 2,6-bis(tetrazol-4-yl)pyridines (**pytz**), and most importantly 2,2',6,2''-terpyridine (**terpy**), Scheme 1, all of which have been exploited for a host of applications. **Btp** is a relatively recent addition to this family of terdentate ligands; being a highly synthetically versatile building block, it complements the aforementioned ligands, with respect to shape/structure, physical, and coordination properties. However, in contrast to the aforementioned systems, **btp** ligands can be easily synthesised in relatively high yielding and facile reactions by exploiting Cu(I)-catalysed azide–alkyne cycloaddition (CuAAC) chemistry. Therefore the synthesis is amenable to a wide range of functional groups as we will discuss below, making derivatives of this ligand highly attractive targets for



⁶⁰ Scheme 1 A selection of pyridine-centred terdentate binding motifs attested in the literature.

supramolecular and materials applications. Consequently, it offers a new and novel means to generate both structurally simple coordination complexes as well as more complex and novel supramolecular self-assembled architectures, and materials.

However, before embarking on a discussion of such **btp**-based systems, it is worth highlighting some of the examples in which the aforementioned terdentate coordinating ligands have been employed. Of these, the **dpa** ligand and its derivatives have been well studied over the years, particularly for their use in the formation of luminescent supramolecular self-assemblies with Ln(III) ions, by researchers such as Bünzli, Piguet and Chauvin and their co-workers.¹⁻⁷ Chauvin *et al.* have proposed the use of Cs₃[Ln(**dpa**)₃] complexes as secondary standards for luminescent quantum yield determination.^{8,9} **Dpa** ligands have also been studied for their interactions with transition metal ions,¹⁰ and in particular amide derivatives of **dpa** have been studied extensively, including for use in the formation of transition metal-containing interlocked systems,¹¹⁻¹³ as a ligand in Cu(II)-promoted hydroxylation of THF¹⁴ as well as coordination chemistry with Ln(III) ions.¹⁵ Our own research group has recently employed such amide derivatives of **dpa** in the formation of highly symmetrical and chiral luminescent bundles,¹⁶ helicates¹⁷ and half-helicates¹⁸ templated *via* Ln(III)-directed self-assembly. We have also employed **dpa** in the fabrication of chiral luminescent Langmuir-Blodgett films, which emit in the red and near infrared regions of the electromagnetic spectrum.^{19,20} Earlier this year, we demonstrated the potential of **dpa** as a central core for the generation of [2]- and [3]-catenanes, which to the best of our knowledge, are the first examples of the use of Ln(III)-directed synthesis of such interlocked structures.²¹

Related to the **dpa** ligands are the **pybox** ligands, which can in fact be prepared from **dpa**. As with **dpa** these ligands have been employed as sensitisers for Ln(III) ions,²²⁻²⁴ and as suitable ligands in asymmetric catalysis (for a useful review of **pybox** in this context, see Desimoni *et al.*²⁵). Recently, the group of de Bettencourt-Dias has also reported the preparation of water-soluble **pybox** sensitisers for Ln(III) luminescence, demonstrating the versatility in its use in coordination chemistry.²⁶

Bpp ligands have been reported as synthetically versatile planar tridentate ligands.²⁷ Two recent reviews by Halcrow concern the coordination properties of **bpp** and related ligands, particularly with respect to their spin-crossover, self-assembly and catalytic applications.^{28,29}

Various structural isomers of 2,6-bis(triazolyl)pyridines, other than the motif upon which this review focuses on, such as the **3**- and **5-btp'** ligands, Scheme 1, have been employed as coordination ligands for transitional metal ions with different applications in mind, *e.g.* determining structural and electronic properties of Ni(II) and Fe(II),³⁰ enhancing the luminescence properties of Ru(II) complexes,^{31,32} forming highly emissive Pt(II) complexes,³³ as well as for the preparation of Os(II)-based light absorbing complexes for solar cell applications.³⁴ Formation of Ln(III) based complexes was also reported.³⁵ Structural isomers prepared from 2,6-azidopyridines have also been attested,³⁶⁻³⁹ recently showing some promise as anion receptors.⁴⁰

Related to the **btp** ligands are the **pytz** systems; a pyridine-

containing binding unit flanked by five-membered tetrazole rings at the 2,6-positions. These ligands have been reported as potential sites of transition metal coordination,^{41,42} as well as (in deprotonated form) as antennae for sensitising Ln(III) luminescence.^{43,44} As for **btp** ligands, **pytz** systems are synthesised *via* 'click' chemistry.

The final ligand to be discussed here is the **terpy** motif, which is ubiquitous in the literature, particularly with respect to the photophysical applications of its Ru(II) complexes,^{45,46} but also other areas, such as materials research,⁴⁷ fabrication of dye-sensitised solar cells,⁴⁸ formation of metal complex wires for electron transport,⁴⁹ DNA and protein binding,^{50,51} formation of metallo-supramolecular coordination polymers⁵² luminescent supramolecular gels,⁵³ and in ion sensing.⁵⁴⁻⁵⁶ It is a truly well-known and loved ligand, which has been employed in coordination chemistry as one of the gold standards. Despite its prevalent use in Ru(II) chemistry, bis-terdentate complexes, such as [Ru(**terpy**)₂]²⁺ are often virtually non-luminescent at room temperature due to thermal population from the ³MLCT (metal-to-ligand charge transfer) to a close-lying non-emitting MC (metal centred) excited state. In order to overcome this, it has been reported that modifying the ligand structure raises the energy of the MC state, for instance by obtaining perfect octahedral geometry leading to a strong ligand field, and hence an increase in luminescence.⁵⁷ We have in the past used the **terpy** ligands for the formation of mixed supramolecular *f-d* metal ion hybrids, where we have employed the ligand as an appendant arm on cyclen (1,4,7,10-tetraazacyclododecane) complexed Ln(III) structures (we also employed this *f-d* metal ion hybrid strategy for the recognition of nucleic acids).^{56,58}

So how well does the **btp** ligand compare to these classical examples listed above? Flood *et al.* pointed out, when first investigating the **btp** motif, that **btp'** (containing 1,2,4-triazoles) had been extensively studied as a coordination ligand.⁵⁹ For instance, Vos and co-workers incorporated such a **btp'** ligand as ligand L into a complex of the form [Ru(**terpy**)L]²⁺ and saw a 300-fold increase of the lifetime of this complex relative to [Ru(**terpy**)₂]²⁺ as a result of raising the ³MC states following the replacement of the weak field **terpy** ligand by a strong σ -donor ligand.³¹

It has also been shown that the **btp** motif has very similar binding properties to **terpy**, with similar bond angles and lengths determined for Ru(II) complexes by X-ray diffraction; as illustrated in Fig. 1. Therefore study of systems such as these is highly valuable; there is still a need in coordination chemistry to explore the development of novel ligands as **terpy** analogues, for a variety of applications. Given the fact that the **btp** ligand can be readily derivatised at the 1-position of the triazole units, this ligand is an excellent candidate for such endeavours.^{60,61} This is further fuelled by the rapid developments that have occurred

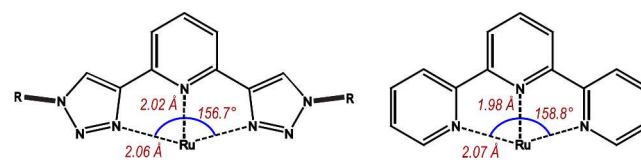


Fig. 1 Comparison of average bond lengths and angles for **btp** and **terpy** chelating motifs, from X-ray crystal structure analysis. Data from references ⁶¹ and ⁶² respectively.

within the field of metallo-supramolecular chemistry. Here, most architectural shapes and topologies have been accessed; hence, the focus has increasingly moved towards developing new methods for functionalising ligands, and synthesis that is modular, facile and high-yielding. The CuAAC reaction, yielding 1,2,3-triazoles, is an obvious candidate which fulfils these criteria. Being central to the synthesis of the structures presented in this review, it is important to highlight some of the key features of this reaction, which we do below. The development of triazole-based structures using 'click' chemistry has recently been reviewed in detail by Schubert *et al.* and we direct interested readers to that comprehensive review for more detailed discussion on its application.⁶³

1.2 1,2,3-Triazoles and the CuAAC 'click' reaction

A challenge for the synthesis of metal-coordinating compounds, identified by Schibli *et al.* in a recent perspective article, is to discover strategies which can give access to wide ranges of ligands with reduced synthetic complexity and preparation, allowing modular synthesis of diverse metal-chelators.⁶⁴ Clearly, 'click' reactions are ideal candidates to fulfil these criteria.

'Click chemistry' is a term first coined by Sharpless and co-workers^{65,66} to describe modular, high-yielding reactions which are ideally insensitive to the presence of oxygen and water. The azide-alkyne 1,3-dipolar cycloaddition (or the 1,3-Huisgen reaction⁶⁷) was identified as the 'cream of the crop' of 'click' reactions. Despite this reaction being known first reported in 1893⁶⁸, the non-selective formation of both 1,4- and 1,5-substituted 1,2,3-triazoles led to minimal applications of these compounds. This setback was largely overcome by the development of the CuAAC reaction^{66,69} which is a regioselective, high yielding and tolerant reaction, exclusively giving 1,4-disubstituted 1,2,3-triazole products.^{70,71} Both the azide and alkyne groups, which form the substrates for the CuAAC reaction, have a wide range of advantages. Both are stable in the presence of nucleophiles, electrophiles, solvents and molecular oxygen, which are common under standard reaction conditions. In addition, both functionalities can be easily introduced into organic compounds,⁷² the azide by reaction of sodium azide with organic halides, or by converting primary amines into azides through the use of simple catalysts (allowing for the use of chiral amines in easy synthesis), while the alkyne moiety can be introduced, for instance, *via* Sonogashira coupling reactions.

The majority of reported uses of the CuAAC reaction have not taken advantage of the coordinative abilities of the 1,2,3-triazole motif, rather employing it as a linker between other functional building blocks, such as their use in coupling Ln(III) cyclen complexes to redox-active motifs,⁷³ carbohydrate building blocks⁷⁴ or another Ln(III) cyclen complex⁷⁵ an area of research developed by Faulkner *et al.*, Hudson and co-workers and our own research group, respectively, for application in sensing and imaging. The CuAAC reaction has also been used to 'click' modifications onto the 4-pyridyl position of terdentate ligands, such as **dpa** derivatives in order to synthesise metal chelators,⁷⁶ form Ln(III) luminescent probes,⁷⁷ and graft these onto silica nanoparticles.⁷⁸

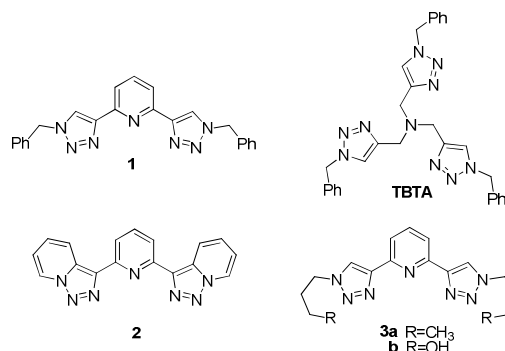
There are many review articles covering this area, such as the use of the CuAAC reaction in construction of dendrimers and

polymeric architectures,⁷⁹ modification of peptidomimetic oligomers,⁸⁰ and construction of higher order interlocked supramolecular structures.⁸¹ Schibli *et al.* described the installation of triazolyl metal chelating sites into molecules in a single step using the CuAAC reaction as the 'click to chelate' approach.⁸² It is worth noting that due to its relative planarity and strong dipole moment, the 1,2,3-triazole has a physicochemical resemblance to the amide bond, explaining its use as a linker in biological, biochemical and carbohydrate research,⁸³ as well as interest in 1,2,3-triazole hydrogen bonding behaviour in anion supramolecular chemistry, which has been reviewed by Hua and Flood.⁸⁴

Although there have been a number of recent overviews of metal-chelating systems synthesised using the CuAAC reaction,^{64,85,86} as a result of the rapid and recent explosion of interest in the terdentate 2,6-bis(1,2,3-triazol-4-yl)pyridine motif (**btp**), only limited examples of ligands containing this motif have been included.^{59,71,87,88} The objective of this review, as stated above, is to address this deficit, detailing the chemistry and the applications of **btp** ligands which have been reported in the literature over the last few years.

1.3 The btp motif

The **btp**† motif combines the favourable features of a pyridine-centred terdentate binding site with the coordinating ability of the 1,2,3-triazole, along with its ease of preparation *via* CuAAC chemistry. The first instance in the literature of the **btp** motif, ligand **1**, was presented in work by Fokin and co-workers in 2004 as part of a library of 1,2,3-triazole-containing ligands designed to stabilise Cu(I) and increase the rate of the CuAAC reaction,⁸⁹ the very reaction that was used to prepare these ligands (a number of 1,2,3-triazole-containing ligands had previously been reported for stabilising various metal ions for catalysis⁶⁴). The benzyl-substituted ligand **1** was reported as facilitating increased yields in the reaction, however, **TBTA** performed better. In the same year, another **btp**-containing structure **2**, reported by Abarca and co-workers was designed to act as a polynitrogenated potential helixating ligand.⁹⁰ The proposed structure of a fused aromatic system, however, was not synthesised *via* the CuAAC reaction (*vide infra*).

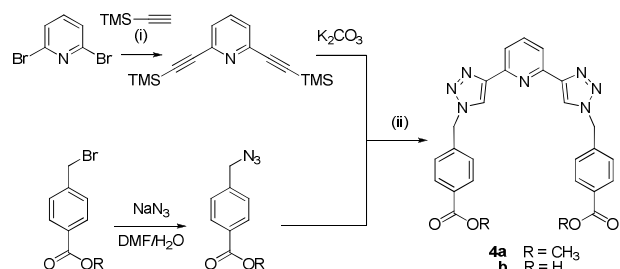


In 2007, Flood and co-workers reported the interactions of **btp**-containing ligands **3** with metal ions, including Fe(II), Ru(II) and Eu(III), and showed that these ions could form stable coordination compounds with **3**.⁵⁹ This research demonstrated that synthesis of the **btp** based ligand provided easy access to a class of terdentate ligands, possessing a **terpy**-like coordination

environment, but with distinctive differences such as the broad scope of functionalisation available *via* the CuAAC reaction and size differential between the heterocyclic rings. Hence, **btp** provides a promising method of introducing **terpy**-like functionality to macromolecules because of the excellent feasibility of azide substitution and ‘click’ chemistry,⁶⁰ as was also discussed above.

1.3.1 Synthetic strategies

As discussed above, the CuAAC reaction is versatile and tolerant to a wide range of substrates and solvents. Reported syntheses of **btp**-containing molecules are almost all performed by undertaking such a reaction or a variant of it, with a range of substrates and solvent systems. Generally, the synthesis is achieved upon reaction of an organic azide with a 2,6-diethynylpyridine (either protected or not, as discussed below) in the presence of Cu(I), obtained from either a Cu(I) salt (*e.g.* CuI) but more commonly from a Cu(II) salt reduced *in situ*, (*e.g.* CuSO₄). We have found a one-pot synthesis such as that shown in Scheme 2 ideal for the formation of ligands **4** in moderate yields and high purity.⁶¹ The scope of azides and alkynes used as substrates for these reactions are discussed in the following sections, as well as methods for obtaining **btp** ligands derivatised at the 4-pyridyl position and asymmetrical ligands. The versatility of triazolyl substituents reported is remarkable, with alkyl chains of various lengths, aryl groups and even motifs such as ferrocenes⁹¹ and porphyrins⁷¹ being introduced. **Btp** ligands have even been attached directly to surfaces, such as polystyrene,⁶⁰ and bound to TiO₂ surfaces;⁹² clearly demonstrating the wide scope such ligands have in modern coordination and supramolecular chemistry.

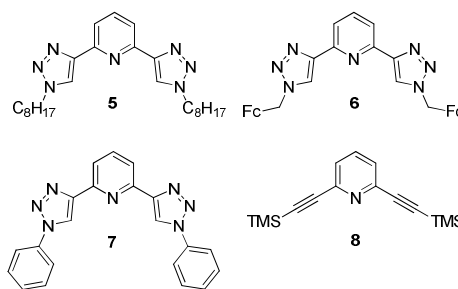


Scheme 2. CuAAC synthesis of ligands **4**. (i) CuI, Pd(PPh₃)₂Cl₂, NEt₃/THF; (ii) CuSO₄·5H₂O, Na ascorbate, DMF/H₂O.

1.3.2 Azides

The chemistry of azides is well-established and an endless number of variants can be synthesised according to the requirements of the research. Azide compounds, however, particularly low-weight organic azides, can be hazardous to handle when isolated, due to the potential explosive nature of compounds where $(N_C + N_O)/N_N \leq 3$, and hence appropriate care should be taken. A number of research groups have, therefore, developed protocols to generate the azide substrate for the CuAAC reaction *in situ* from the halide precursor and use it immediately. For example, Crowley *et al.* have reported a number of compounds, such as **1**, **5**, **6** and **7**, that can be synthesised by a ‘one pot multi-component CuAAC ‘click’ approach’.⁹¹ Here, the authors have taken advantage of the convenience of introducing azide functionality into organic halides upon stirring with sodium azide in order to introduce a diverse range of groups, such as alkyl chains, ferrocenyl groups and aryl groups. While

compounds **1**, **5** and **6** can all be prepared under the same conditions and at room temperature in a DMF–water (4:1) mixture, the aryl azide **7** required more forcing conditions by refluxing in an aqueous ethanol mixture.



1.3.3 Alkynes

Of necessity, to form **btp** systems, the alkyne substrate for these reactions must be some derivative of 2,6-diethynylpyridine. For most **btp** ligands discussed herein, which do not contain a substituent in the 4-position of the pyridine ring, the 2,6-diethynylpyridine substrate was prepared upon performing a Sonogashira coupling between 2,6-dibromopyridine and (trimethylsilyl)ethyne furnishing the protected species **8** (other silylalkynes, such as triisopropylsilyl groups, have also been reported⁷¹). The protected alkyne can either be deprotected before use (treating with a base, *e.g.* K₂CO₃,^{93,94} KF,⁹⁵ or KOH^{87,96}) or used directly in the CuAAC reaction, as shown in Scheme 2.

Fletcher *et al.* reported a one-pot deprotection/‘click’ paradigm for the synthesis of a range of triazole-ligands, which provided near quantitative and selective transformation of trimethylsilyl-protected terminal alkynes and organic azides to the desired 1,2,3-triazole-containing products.⁹³ K₂CO₃ was included with the substrates in the reaction and the *in situ* deprotection step was reported to be the rate-determining step, since only triazole products and trimethylsilyl-protected alkynes were observed in reaction mixtures, never free terminal alkyne intermediates. This paradigm removes the necessity for purification of the intermediate terminal alkyne, and hence, in the pursuit of new **btp**-derivatives, it would be expected that this methodology would be incorporated into an optimised synthetic approach.

1.3.4 Solvents and workup

Another great advantage of ‘click’ reactions is that they can be carried out under aqueous conditions, which is convenient, cheap and environmentally preferable. As such, it is no surprise that the vast majority of CuAAC reactions reported for the synthesis of **btp**-ligands were carried out in aqueous media. Solvent choice has relatively little effect on yields, and it appears to be a matter of preference and, sometimes, solubility of starting materials that determines the choice of solvent systems. Alcohols like ethanol^{87,95,97,98} and *tert*-butyl alcohol^{93,94,96} mixed with water are most common in the literature, while DMSO (with⁹⁹ or without¹⁰⁰ water), THF,⁶⁰ CH₃CN¹⁰¹ and DMF^{70,91} are also attested.

Reviewing the literature shows a few common approaches to purifying the **btp** products. If the product precipitates from the reaction mixture it is simply isolated by filtration and purified by chromatography, otherwise the reaction mixture was concentrated and then purified upon use of chromatography. Alternatively, the treatment of the crude reaction mixture with a basic solution of an EDTA salt, in order to scavenge Cu(I) ions, has also been

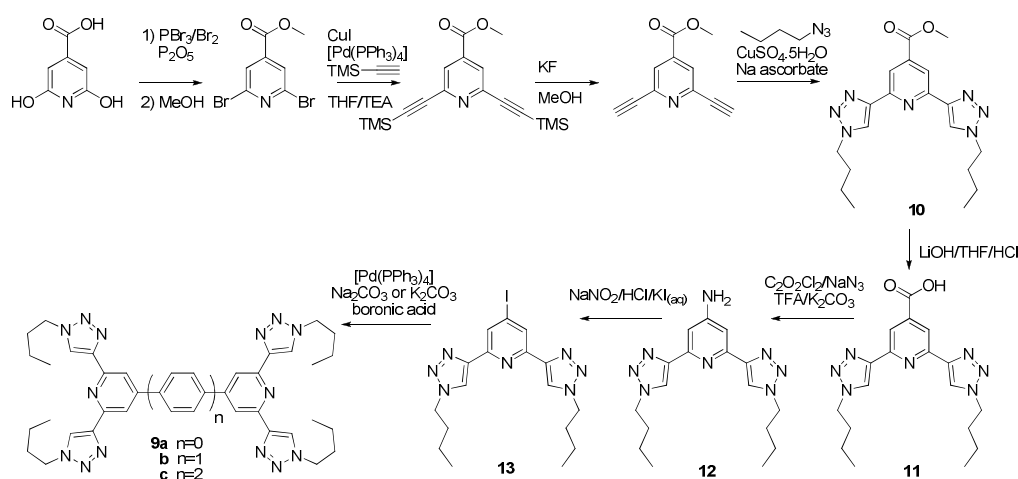
demonstrated, resulting in isolation of the desired product upon extraction into organic solvent and, if necessary, purification by chromatography.

1.3.5 Functionalising the 4-pyridyl position

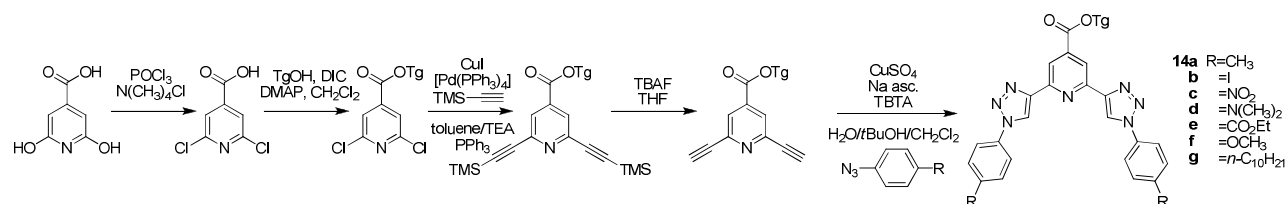
Chandrasekar and Chandrasekar described a method for functionalising **btp** motifs in the 4-pyridyl position in their work on developing ditopic ligands **9** (Scheme 3).¹⁰² This strategy used citrazinic acid as a starting point,¹⁰³ which is brominated and converted into a methyl ester before introducing the alkyne functionality using the Sonogashira coupling discussed above and subsequently deprotecting the alkyne. The alkyne was used as a substrate for a CuAAC reaction, yielding **10**; saponification of the ester with LiOH gave **11**. Sequential conversion of the carboxylic acid into an acyl azide followed by thermal Curtius rearrangement and succeeding hydrolysis of the trifluoroacetamide provided the amino derivative **12** in good yield. Diazotisation of this compound, followed by reaction with KI produced iodide derivative **13**. The resulting iodide was

reacted with either bis(pinacolato)diboron to give directly-linked ditopic **btp** ligand **9a**, or aryl boronic acids to introduce mono- and diphenyl linkers, giving **9b–c**. Hecht and co-workers introduced an ester functionality in a different way: transforming citrazinic acid into a dichloro-derivative before introducing a 3,6,9-trioxadec-1-yl (Tg) ester functionality into the 4-pyridyl position of ligands **14** as shown in Scheme 4.⁷¹

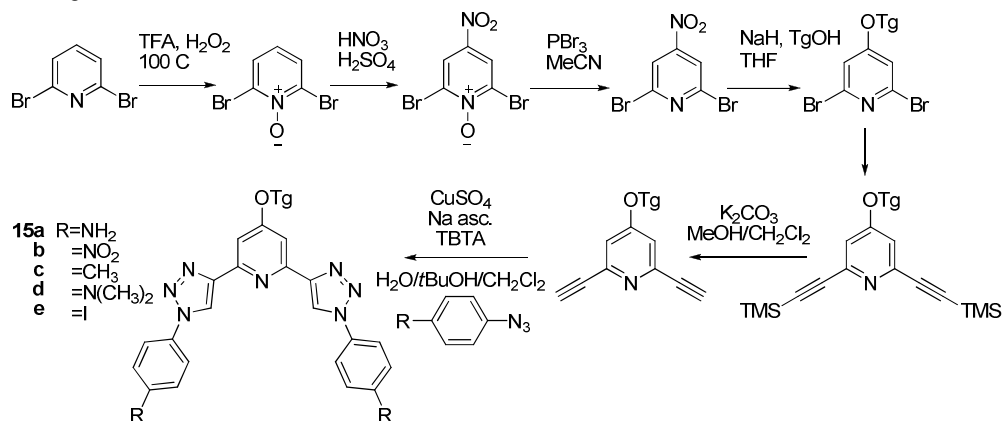
An alternative approach for introducing a substituent onto the pyridyl ring, shown in Scheme 5, has exploited the ease of nitration of 2,6-dibromopyridine-*N*-oxide and allowed the introduction of ether chains to ligands such as **15**.^{71,88,104} Finally, Schubert and co-workers have demonstrated a strategy, using a selective Sonogashira coupling to 2,4,6-tribromopyridine, a general scheme of which is shown in Scheme 6 to introduce alkyne-containing linkers into the 4-position of **16**, yielding ditopic ligands like **17**.^{95,105,106}

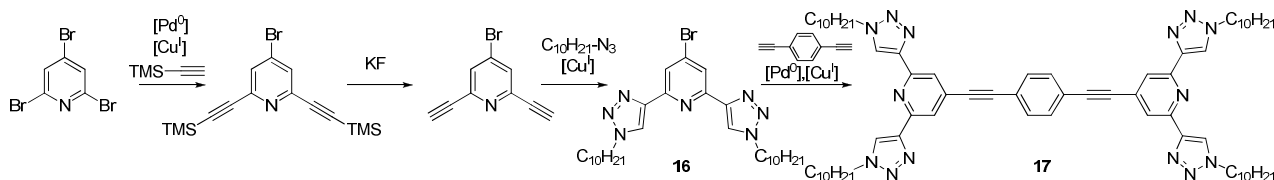


Scheme 3 Synthesis of ditopic 'back-to-back' ligands **9a–c**.¹⁰²



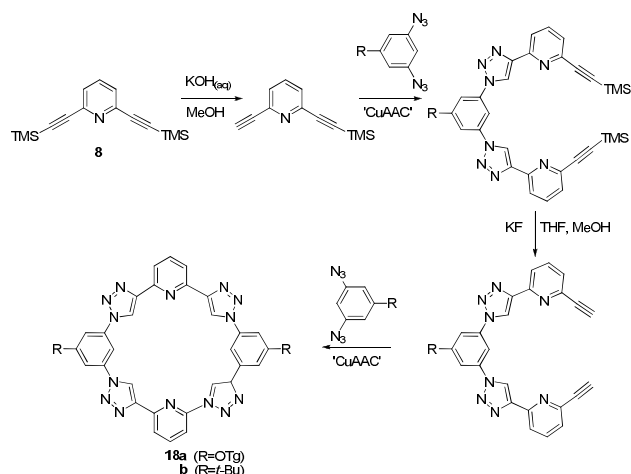
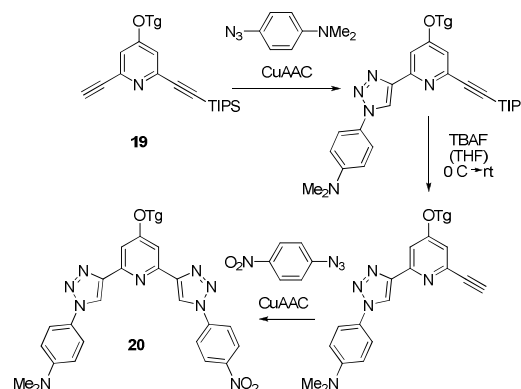
Scheme 4 Synthesis of ligands **14**.



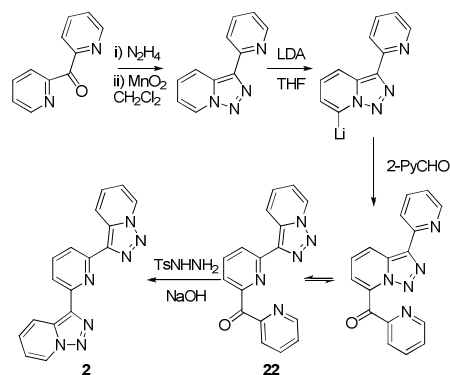
Scheme 5 Ether functionalisation⁷¹, yielding ligands **15**.**Scheme 6** Functionalisation at the 4-pyridyl position with alkyne-containing linker, yielding ligand **17**.**1.3.6 Stepwise ‘click’ reactions and asymmetric btp ligands**

Several examples of btp ligands have been reported to date where it has been necessary to synthesise the **btp** core in a stepwise fashion, using several ‘click chemistry’ reactions. An example of such a ligand is that of Flood and co-workers, who prepared the ‘triazolophane’ macrocycles **18** for encapsulation of halide ions, Scheme 7.⁸⁷ This stepwise method avoids the possible polymerisation reactions that could occur in a one-pot synthesis. This approach required mono-deprotection of **8** by stirring for 30 minutes with KOH before purifying the desired compound by column chromatography. This type of stepwise preparation has also been employed by Hecht and co-workers to prepare asymmetric **btp** compounds, as shown in Scheme 8. Here, a 4-substituted 2,6-dibromopyridine initially underwent a Sonogashira coupling with triisopropylsilyl-ethyne (TIPS-ethyne), after which one TIPS group could be selectively removed upon reaction with TBAF, yielding **19** with one alkyne available to the ‘click’ reaction with a particular azide.

Subsequent removal of the other TIPS group allowed for substitution of a different azide, leading to **btp** ligand **20** with non-identical ‘arms’.⁷¹ A similar approach was reported to produce helically folding poly-**btp** compounds **21** by bidirectional growth with repetitive sequences of coupling monomers followed by deprotection of terminal alkynes.⁸⁸

**Scheme 7** Synthesis of triazolophanes **18** from **8** via stepwise ‘click’ reactions.**Scheme 8** Synthesis of asymmetric **btp** ligand **20**, from **19**.**1.3.7A non-‘click’ synthetic strategy**

Only five molecules containing the **btp** motif have been reported which were not synthesised *via* the CuAAC reaction. Work published by Abarca and co-workers showed the unexpected synthesis of a symmetrical ligand **2** upon reaction of ketone **22** with tosylhydrazine in NaOH, due to triazolopyridine–pyridine ring rearrangement as shown in Scheme 9.^{90,107,108} Other ligands containing varied fused ring systems were prepared in a similar manner from different ketones.¹⁰⁸

**Scheme 9** Non-‘click’ synthetic approach to a **btp**-containing fused system **2**.**1.3.8 Conformational switching of btp with cations and anions**

The C–C bond connecting the pyridyl and triazolyl moieties of **btp** allows for free rotation, however, preference has been shown for different conformations under various conditions, as demonstrated in Fig. 2. Coordination of this terdentate motif to metal ions results in a dramatic conformational switching in these ligands; the free ligands display the triazole moieties *anti-anti* (or *kinked*) with respect to the pyridyl nitrogen atom. This is

evidenced in the solid state by various X-ray crystal structures in the literature.^{91,96,109-111} Due to favourable electrostatic interactions the *anti-anti* conformation of the **btp** core dominates in solution at neutral pH, while repulsion between nitrogen lone pairs destabilises the alternative. NOE NMR experiments have shown that interactions between pyridyl and adjacent triazolyl protons are practically non-existent, but upon protonation, medium strength interactions are observed between these protons.⁷¹ In the presence of a cation, such as metal ions or a proton, the *syn-syn* (or 'extended') conformation is observed. This is again borne out in the solid state by a host of X-ray crystal structures of metal complexes.^{59,61,71,91} This sensitivity to the presence of cations can be utilised to create nanoswitches sensitive to either metal ions¹⁰¹ or pH changes.^{96,112}

In contrast to this, coordination compounds with anions all display **btp** in the *anti-anti* conformation,^{87,88} the ability of the acidic triazole CH to hydrogen bond with anions being largely responsible for this conformation. Specific systems featuring this conformation will be discussed in Section 3.

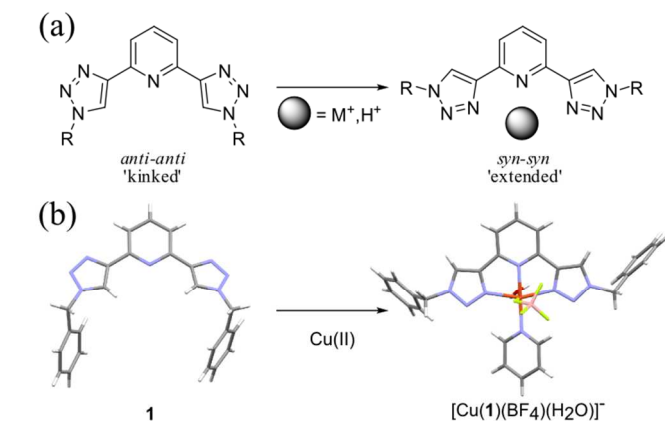


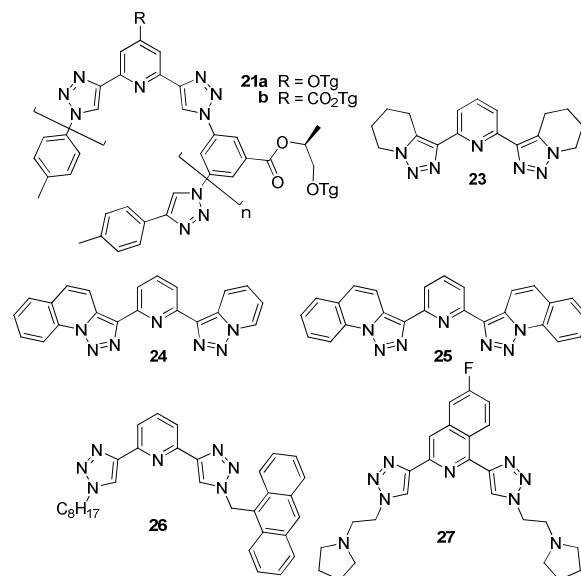
Fig. 2 (a) Demonstration of conformational switching of the **btp** motif; (b) ligand **1** and its Cu(II) complex shown as examples of this switching.⁹⁶

2. Metal coordination chemistry

The coordination of **btp**-containing ligands has been reported with a range of transition metal and lanthanide ions. An overview of this metal coordination behaviour is given below, metal by metal. Interesting characteristics and properties of these systems, such as photophysical, magnetic, electrochemical, structural, sensing and materials applications, are also detailed.

2.1 Nickel

We have reported the molecular structure of the paramagnetic Ni(II) complex $[\text{Ni}(\mathbf{4a})_2](\text{PF}_6)\text{Cl}$, prepared upon reaction of **4a** with $\text{NiCl}_2 \cdot x\text{H}_2\text{O}$ under microwave irradiation.⁶¹ The complex displayed a distorted octahedral geometry and signals in the ¹H-NMR (600 MHz, CD₃CN) spectrum were broadened and shifted as a result of the metal ion's paramagnetism. To the best of our knowledge, this is the only example of a Ni(II)-**btp** complex.



2.2 Copper

As discussed previously (Section 1.3), the first **btp** ligand synthesised, **1**, was employed as a stabilizing ligand for Cu(I) to increase the rate of the CuAAC reaction.⁸⁹ Sankararaman *et al.* obtained a crystal structure of this ligand and also its Cu(II) complex $[\text{Cu}(\mathbf{1})(\text{BF}_4)(\text{C}_5\text{H}_5\text{N})(\text{H}_2\text{O})](\text{BF}_4)$ (see Fig. 2). This work demonstrated the two different conformations adopted by the ligand when isolated (*anti-anti*) and when coordinating a metal (*syn-syn*), as discussed in Section 1.3.8. The geometry about the Cu(II) ion was described as distorted octahedral with the pyridine and triazole moieties nearly in the same plane (with a dihedral angle of 7.5(2)° between the two triazole rings). It was also shown that ligand luminescence was quenched upon complexation.⁹⁶

Crowley and co-workers reported $[\text{Cu}(\mathbf{1})\text{Cl}_2]$.⁹¹ The complex adopted distorted square pyramidal geometry and the authors noted with interest that the structure was very similar to that reported for an analogous **terpy** complex.¹¹³

Ligand **2**, its derivative **23** and related compounds **24** and **25**, prepared by Abarca and co-workers were all fluorescent. Upon addition of Cu(II) to solutions of these compounds in a 98:2 ethanol-water mixture, emission was dramatically quenched, allowing these compounds to be considered as 'switch-off' chemosensors for Cu(II).¹⁰⁸ The X-ray crystal structure of $[\text{Cu}(\mathbf{2})(\text{H}_2\text{O})_2(\text{BF}_4)]\text{BF}_4 \cdot 2\text{H}_2\text{O}$ was analysed in detail in order to understand the role π - π stacking might play in magnetic exchange between paramagnetic Cu(II) centres, as well as contributions from ferromagnetic coupling along hydrogen bonds. Thermal variation of $\chi_{\text{m}}T$ (molar magnetic susceptibility per Cu(II) ion times temperature) yielded data which suggested the compound presented weak ferromagnetic coupling. It was concluded that magnetic exchange through the hydrogen bonds was the most likely pathway.¹¹⁴

Both Zhu and Dash briefly mentioned Cu(II) quenching the fluorescence emission of ligands **5**, **26**¹¹⁵ as well as compound **27**.¹¹⁶ However, these systems will be discussed in more detail below in relation to their fluorescence emission enhancement upon interaction with Zn(II).

2.3 Zinc

The interactions of the fused-ring ligand **2** with Zn(II) have been studied.¹⁰⁷ Both $[\text{Zn}(\mathbf{2})]^{2+}$ and $[\text{Zn}(\mathbf{2})_2]^{2+}$ stoichiometries were observed by mass spectrometry and suitable crystals for X-ray diffraction studies were obtained of the bis-ligand complex (see Fig. 3(a)). The addition of $\text{Zn}(\text{ClO}_4)_2$ to solutions of the fluorescent ligand in a 98:2 ethanol–water solvent mixture showed significant chelation enhancement of fluorescence. This was in contrast to the quenching effects observed upon addition of other divalent transition metal ions, such as Cu(II) as mentioned above. This Zn(II) complex was examined as a suitable fluorescence chemosensor for monovalent anions (*vide infra*, Section 3). Similar chelation enhancement of fluorescence was also observed for unsaturated ligand **23** and, to a lesser extent, for compounds **24** and **25**, however, their behaviour with anions has not been investigated to best of our knowledge.¹⁰⁸

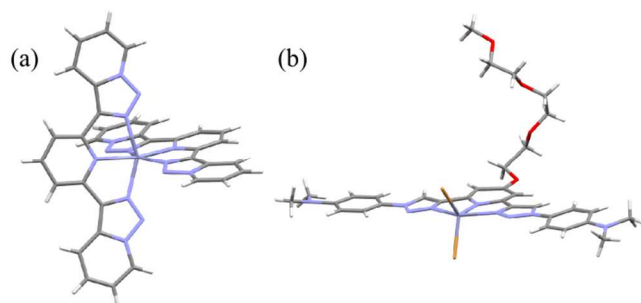


Fig. 3 (a) Zn(II) complex with **2**. Solvent molecules and counterions have been omitted for clarity¹⁰⁷. (b) Molecular structure of $[\text{Zn}(\mathbf{15a})\text{Br}_2]$. Co-crystallised ZnBr_2 molecules and solvent molecules have been omitted for clarity.

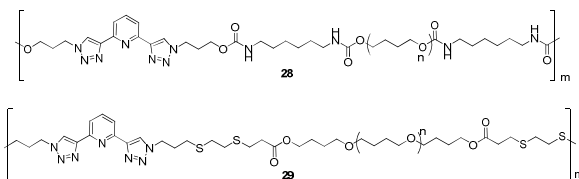
Hecht and co-workers published the molecular structure of the monoleptic Zn(II) complex $[\text{Zn}(\mathbf{15a})\text{Br}_2]$, see Fig. 3(b), in which the Zn(II) coordination sphere was described as being a distorted square pyramidal geometry.¹¹¹ In separate work, Meudtner and Hecht briefly reported the formation of metallo-supramolecularly crosslinked gels from **btp**-containing polymers **21** upon addition of Zn(II).¹⁰¹ However, this work has not, to the best of our knowledge, been followed up by the authors. However, Yuan *et al.* also produced gels upon addition of stoichiometric amounts of $\text{Zn}(\text{CF}_3\text{SO}_3)_2$ solutions to different **btp**-containing polymers **28** and **29** which demonstrated fluorescence under UV light irradiation and remarkable self-healing properties.^{117–119} These gels showed little change in emission as a function of temperature, but displayed potential for chemosensing, since a number of chelating chemicals tested (*e.g.* **bipy**) caused deconstruction of the gel. These systems will be discussed in more detail in Section 5.6.

Zhu and co-workers are interested in the development of fluorescent ligands for the determination of intracellular Zn(II) concentrations and flux. In contrast to the monoleptic system formed under similar conditions for ligand **15a**, dileptic complex $[\text{Zn}(\mathbf{5})_2][\text{ZnCl}_4]$ was isolated from an equimolar mixture of ligand and ZnCl_2 . The authors suggested that the lack of aryl ‘arms’ (and hence, π - π interactions) made the dileptic system favourable in the solid state for this octyl-substituted **btp** ligand. The ligand displayed the characteristic conformational change upon formation of the complex, which adopted a distorted octahedral geometry in the X-ray crystal structure. ITC and ^1H NMR studies

suggested the formation of strong dileptic complexes of **5** in solution, with the monoleptic complex only being formed at higher Zn(II) concentrations.

Coordination of Zn(II) to asymmetric anthryl ligand **26** caused a 10 nm bathochromic shift in the absorbance band assigned to the **btp** centre of the ligand indicating formation of the metal complex.¹¹⁵ Here, the anthryl emission was quenched upon addition of Zn(II) as a result of PET from the photoexcited anthryl group to the Zn(II)-bound **btp**; this conclusion was supported by frontier molecular orbital calculations and cyclic voltammetry (CV) measurements.

Dash and co-workers designed the water soluble pyrrolidinyl-appended **btp** ligand **27**, which could detect metal ions.¹¹⁶ A wide range of metal ions were screened, but, as for the examples discussed above, addition of Zn(II) was shown to cause a significant ‘turn-on’ fluorescence response upon formation of a 1:1 complex; Zn(II) giving the greatest enhancement (20-fold) of all the ions tested. The sensor gave 3.2-fold selectivity for Zn(II) over Cd(II), an important result for biological sensing applications, as many Zn(II) sensors often show a high affinity for Cd(II). Moreover the sensor was found to be cell-membrane permeable and responsive to Zn(II) within living cells, such as the human melanoma cell line A375. These results, in conjunction with the quenching response of **27** to the presence of Fe(II) (*vide infra*), were combined to fabricate a molecular logic gate mimic, which will be discussed in more detail in Section 5.2.



2.4 Silver

Significant efforts have been made by both Crowley^{70,91} and Schubert⁹⁷ to prepare Ag(I)-complexes of **btp**-containing ligands. The coordination connectivity of Ag(I) ions with **1** in the solid state has been elucidated by using X-ray crystallography. The results were somewhat unexpected. Elemental analysis indicated that complexes with a 1:1 metal:ligand stoichiometry were formed, with the complex crystallising as a tetrameric tetrasilver cation containing Ag(I) ions which were bridged by various pyridyl and triazolyl nitrogen atoms in the ligand, as shown in Fig. 4, with each Ag(I) ion adopting a distorted tetrahedral geometry.⁹¹

The complexation of Ag(I) with the related ligand **30** was also studied by elemental analysis and mass spectrometry. Elemental analysis suggested that this ligand adopts a 1:1 metal:ligand stoichiometry, however the ESMS spectrum also contains a weak m/z peak corresponding to the $[\text{Ag}_3(\mathbf{30})_2](\text{SbF}_6)^{2+}$ ion, indicating that in solution a Ag(I) ion can bind within the central cavity between the various triazole units of the structure. Such behaviour has also been observed for the analogous 2,6-bis-(1,2,3-triazol-4-yl)benzene ligand, **btb**.⁷⁰

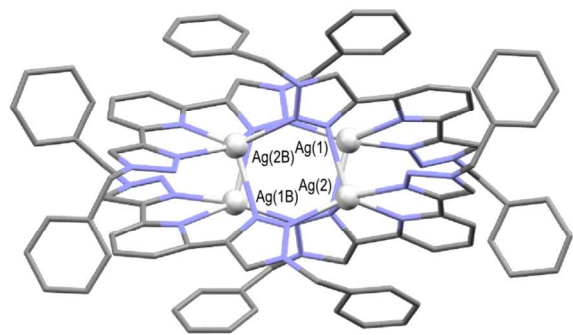
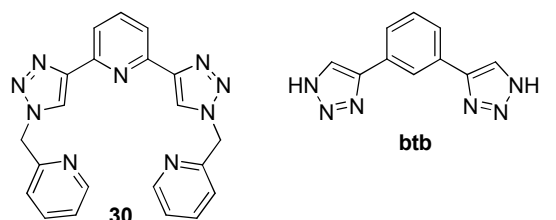


Fig. 4 Molecular structure of tetrasilver cation formed with ligand **1**. Hydrogen atoms, solvent molecules and counterions have been omitted for clarity. Ag(I) atoms are labelled.⁹¹

2.5 Iridium

To the best of our knowledge, our research group has reported the only example of an Ir(III)–**btp** complex, [Ir(**4a**)Cl₃].⁶¹ X-ray crystallography, Fig. 5, revealed that the Ir(III) ion adopted a distorted octahedral geometry, with an N₃Cl₃ coordination sphere.¹⁰ The intraligand triazolyl *trans*-N–Ir–N angle was found to be 159.3(2)°, differing from the ideal angle of 180°. In comparison, the analogous **terpy** complex had a less distorted *trans*-N–Ir–N angle of 161.3(1)°.¹²⁰ At room temperature, this complex displayed a luminescence band centred at 330 nm, while at 77 K, a broad luminescence centred at 450 nm became much more apparent; the fluorescence band at 330 nm being seen as a shoulder in the spectrum. This complex was found to be quite unstable, decomposing over a period of two weeks in solid form,¹⁵ thereby limiting its potential for applications.²⁰

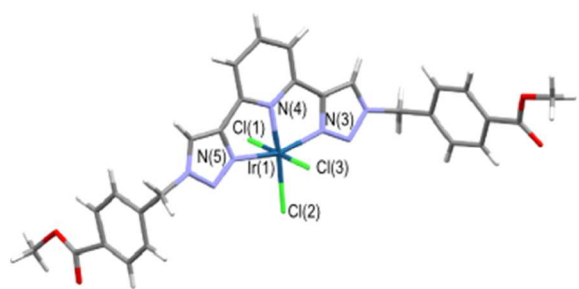


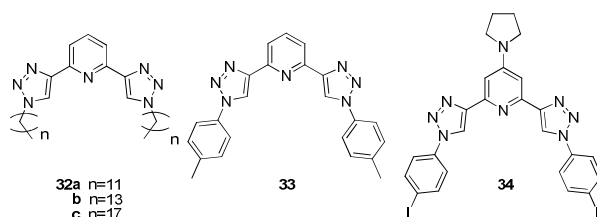
Fig. 5 Molecular structure of [Ir(**4a**)Cl₃]. Solvent has been omitted for clarity.⁶¹

2.6 Platinum

With the aim of developing optoelectronically applicable film-forming metallopolymers, Schubert and co-workers reported the ability of ditopic ligand **31** to form metallopolymers with the Pt(II) ion, as shown in Scheme 10. The racemic and branched

alkyl chains in the ligand were selected to aid solubility of the planar Pt(II)-complexes and deter intermolecular π -stacking.¹⁰⁶ The optoelectronic properties of the metallopolymer were examined, with the complex showing a broad and intense MLCT transition in the visible range, which was red-shifted, and more intense than the individual ligand. No Pt(II)-centred emission was detectable. It was suggested that electronic communication might be possible between Pt(II) centres due to the organometallic Pt(II)-acetylene bond, which leads to ligand contribution to the HOMO.³⁵

Our research group has also reported the formation of Pt(II) complexes with **4a** and **4b**. These complexes displayed only ligand-centred emission in solution at room temperature, but in CH₃CN glasses at 77 K showed behaviour similar to that of **terpy** analogues, resulting in emission due to Pt(II)–Pt(II) stacking interactions as well as interactions between the aromatic ligands.⁴⁵^{61,121}



Yam and co-workers reported the synthesis of a series of chloroplatinum(II) complexes [Pt(**btp**)Cl]X (X=Cl[−], PF₆[−], CF₃SO₃[−]) with ligands **1**, **3a**, **5**, **7** and **32a–c**, as well as a range of related luminescent alkynylplatinum(II) complexes. The chloroplatinum(II) complexes were found to be non-luminescent in solution at room temperature, however, the alkynylplatinum(II) complexes were observed to be luminescent, displaying large Stokes shifts, microsecond lifetimes and an insensitivity to the various alkynyl substituents utilised, leading to the suggestion that emission originated from a [d_{z²}]²(Pt)→ π^* (**btp**) MLCT excited state. Electrochemical measurements of these complexes were also reported. Amphiphilic properties of complexes [Pt(**32a**)Cl]Cl and [Pt(**32a**)(C≡C–C₆H₅)]Cl were studied, showing the ability of these species to form stable and reproducible Langmuir-Blodgett films at the air-water interface.¹²²

2.7 Palladium

Tolyl derivative **33** was developed as a model ligand for polymer synthesis of Pd(II)-containing polymers (discussed in more detail in Section 5.5 below). The crystal structure of this ligand displayed a crystallographic C₂ axis along the centre of the pyridine motif. Reaction with [Pd(cod)Cl₂] yielded [Pd·(**33**)Cl][Pd(DMSO)Cl₃], the only Pd(II) complex of a discrete **btp** system in the literature, of which a crystal structure was also obtained.¹²³

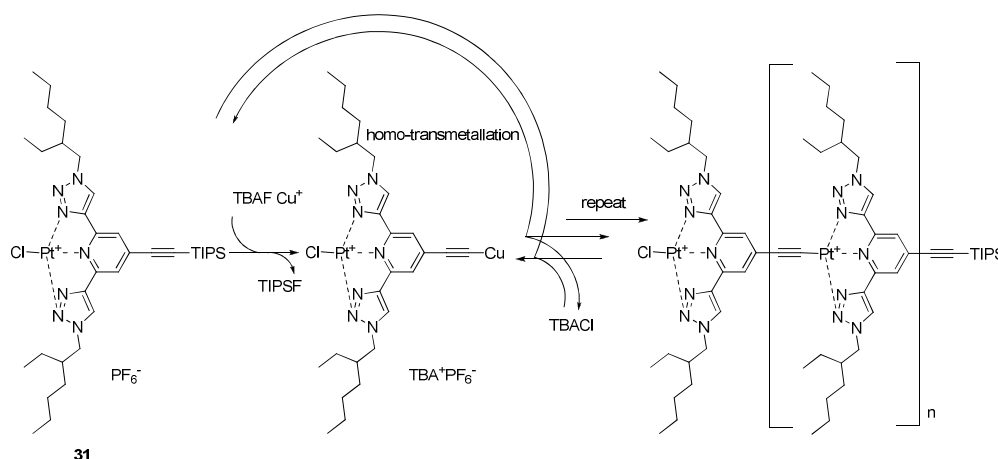
2.8 Lead

Zhu and co-workers investigated the coordination chemistry of two ligands **5** and **26** with Pb(II).¹¹⁵ ¹H NMR titrations of **5** with the metal ion showed the likely formation of the 3:1 complex with chemical shifts suggesting a stronger binding of Pb(II) to the pyridyl nitrogen atoms than the triazolyl, perhaps in a bidentate

Cite this: DOI: 10.1039/c0xx00000x

www.rsc.org/xxxxxx

ARTICLE TYPE



Scheme 10 Preparation of Pt(II) metallopolymer of 31.

manner. Up to 0.5 equivalents of Pb(II), the data suggests that a 2:1 complex was formed with a tridentate binding mode. The behaviour of anthryl ligand **26** with Pb(II) was similar to that discussed above for Zn(II) (Section 2.3), with shifts in the absorbance band assigned to the **btp** centre and a quenching of anthryl emission, probably through an intramolecular PET pathway.

2.9 Iron

Iron complexes of **btp** ligands would be expected to attract significant interest for their magnetic properties, given that spin-crossover behaviour of other terdentate systems has been extensively investigated.¹²⁴⁻¹²⁷ In fact, only one research group has investigated the magnetic behaviour of such systems, with others reporting coordination behaviour, effects of the metal ion on emission intensity and electrochemical properties. These systems will now be discussed.

Flood and co-workers have briefly demonstrated the capability of ligands **3a** and **3b** to coordinate Fe(II).⁵⁹ The UV-vis spectrum of $[\text{Fe}(\mathbf{3b})_2](\text{PF}_6)_2$ displayed both MLCT and LC (ligand-centred) bands that were blue-shifted with respect to the **terpy** analogue; an effect which is attributed to the accessibility of higher energy excited states and the LUMO of the **btp** core being higher energy than that of **terpy**. CV measurements confirmed this hypothesis, showing that the primary differences to the analogous **terpy** complexes were indeed associated with the ligand. CV measurements were also used to observe an increased quasi-reversible oxidation band in this complex upon addition of water. This behaviour was not observed with $[\text{Fe}(\mathbf{terpy})_2]^{2+}$ and was explained by the sterically unhindered 1,2,3-triazoles allowing for the formation of a heptadentate Fe(III) complex following oxidation, with a bound water molecule.

Upon addition of Fe(II) in to aqueous solutions of sensor **27** (discussed above, Section 2.3), fluorescence was quenched,

whereas addition of Fe(III) caused negligible changes in fluorescence.¹¹⁶ Quenching was proposed to occur through a PET or EET (excitation energy transfer) mechanism. This 'switch-off' quenching response was also observed in live cells *in vitro*, allowing for imaging of intracellular Fe(II). The 'switch-off' response observed was coupled with the 'switch-on' response in the presence of Zn(II) for the fabrication of a molecular logic gate, which will be discussed in detail in Section 5.2.

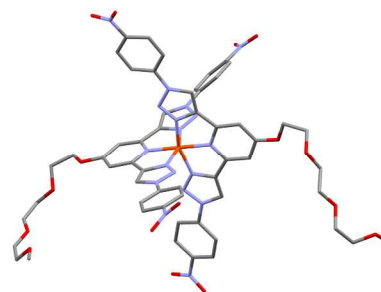


Fig. 6 Molecular structure of $[\text{Fe}(\mathbf{15b})_2](\text{CF}_3\text{SO}_3)_2$. Only one crystallographically independent molecule is shown; hydrogens, counterions and solvent molecules have been omitted for clarity.

Hecht, Limberg *et al.* produced the iron complex of **15a** in order to investigate the ligand field strength of this ligand and compare it with other terdentate ligands. The shorter than expected Fe–N bonds observed in the X-ray crystal structure at 116 K, which is shown in Fig. 6, pointed to a low-spin state iron ion with an average length of 1.93 Å, compared to typical lengths between 2.1 and 2.2 Å for high-spin complexes.⁷¹ This complex showed no thermochromic effects upon warming to room temperature. It was concluded that this ligand's field strength was higher than that of **bpp** and as such, more comparable to that of **terpy**.

Further investigations were undertaken into the magnetic

properties of Fe(II)-complexes of **btp**-ligands **15b–c** and **34**.¹¹¹ When [Fe(**15b**)₂](CF₃SO₃)₂ was heated to 200 °C, the red-brown powder changed its colour to yellow. The red-brown colour was not re-established upon cooling (even at very low temperatures over several days), but could be regenerated by dissolving the complex in CH₃CN. Measurement of $\chi_m T$ over the range of 5–400 K showed a partially reversible hysteresis in magnetic susceptibility between 325 and 400 K. Mössbauer spectra of the red-brown powdered sample were measured at a range of temperatures, and the data showed the predominance of the low-spin state from 7–295 K, while spectra of the yellow (heated) powder showed the predominance of the high-spin state. The conversion was claimed to be quite irreversible. Similar behaviour was noted for other ligands, but with variation in properties dependent on **btp** substituents, with increasing donor character of the ligand decreasing the ligand-field strength.

Hecht and Meudtner also briefly reported the instantaneous formation of metallo-supramolecularly cross-linked gels of **21** upon addition of Fe(II) and other metal ions, but this will be discussed in Section 5.6.¹⁰¹

2.10 Ruthenium

Ru(II) is by far the most abundant transition metal which has been investigated with respect to its coordination chemistry with **btp**-containing ligands, with particular interest arising from the photophysical and electrochemical properties of these complexes.^{59,60,93,95,97,98,100,105,106,111,128,129}

Flood and co-workers showed that Ru(II) forms stable coordination compounds with **3b**. X-ray crystal crystallography showed a 1:2 metal:ligand stoichiometry, with the ligands adopting a distorted octahedral geometry, as demonstrated in Fig. 7(a) for complex [Ru(**3b**)₂](PF₆)₂. The lack of steric interactions was thought to be responsible for these heightened distortions from octahedral symmetry. The effects of coordination on the electronic structure of this ligand also were investigated using UV-vis absorption spectroscopy, where it was shown that the ligand-centred band was blue-shifted ~10 nm upon complexation to Ru(II). When compared to the UV-vis spectrum of the **terpy** complex, both the MLCT and LC bands were blue-shifted but displayed similar band shapes. The optical properties of these complexes were concluded to be similar to their **terpy** analogues, and further studies utilising CV demonstrated that higher energy excited states were accessible as a result of the LUMO of the **btp** core being at a higher energy than that of **terpy**.⁵⁹

A difficulty inherent to Ru(II) polypyridyl complexes is that

tris-bidentate complexes generally show long excited-state lifetimes, but display isomerism, which may be inconvenient. In contrast, bis-terdentate complexes allow formation of linear assemblies without isomerism, but seldom have such advantageous long-lived excited states, due to radiationless deactivation of ³MLCT state through the ³MC state. Variation from the standard **terpy** ligands used in such research may overcome this challenge.^{97,130,131} In a combined experimental and computational study of terdentate CuAAC-derived Ru(II) photosensitisers, the properties of a range of complexes including [Ru(**35**)(**terpy**)](PF₆)₂ and [Ru(**36**)(**terpy**)](PF₆) (where **36** is a cyclometallating **btp** ligand) were compared.¹²⁸ From X-ray crystal structure analysis, it was noted that Ru–N_{pyr} bond lengths were shortened upon cyclometallation. Moreover, DFT calculations suggested that the HOMO of **35** was less destabilised; with almost pure Ru *d*_{xz} character. In contrast, cyclometallation by the phenyl moiety in ligand **36** destabilised the orbitals that are populated in the ³MC states, which are relevant to the radiationless deactivation which is responsible for most [Ru(**btp**)₂]²⁺ complexes being non-luminescent. A photophysical model was presented claiming that while for the complex of **36**, ³MC-ground state intersystem crossing occurs at high energies, for the **btp** ligand, this energy is at low levels and therefore readily accessible. Another approach for reducing radiationless deactivation of Ru(II)–**btp** complexes involves the use of cyclometallating triazolium derivatives, which will be discussed in Section 4.

Hecht and co-workers synthesised a variety of **btp** ligands with different substituents and monitored the effects these variations in the ligand environment had on the properties of the complexes, including a number of Ru(II) complexes.¹¹¹ Substituents represented included electron-withdrawing and donating groups at both the terminal aryl moieties and central pyridine core. The potential applications of complexes with a labile ligand at one coordination site available to bind a substrate for activation during catalysis, for example, led Hecht and co-workers to synthesise a range of 1:1 Ru(II) complexes with **15c–d**, **37** and **38**. Only a crystal structure of [Ru(**37**)Cl₂(DMSO)] was obtained, and showed the ligand binding in a tridentate meridional mode, with two chloride ligands and a DMSO molecule (binding through the sulfur atom) occupying the remaining positions in the distorted octahedral geometry, as demonstrated in Fig. 7(b).¹¹¹

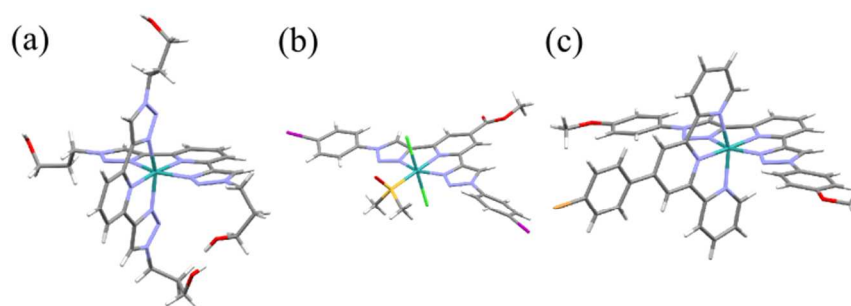
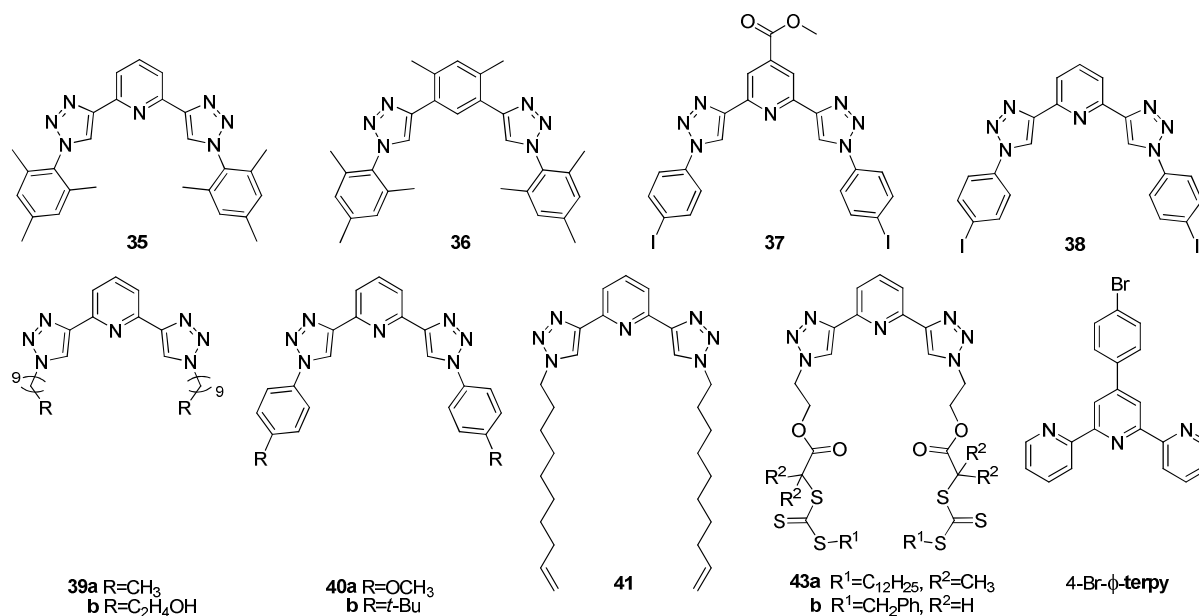


Fig. 7 (a) Molecular structure of [Ru(**3b**)₂](PF₆)₂ showing distorted octahedral geometry. Counterions have been omitted for clarity.⁵⁹; (b) Molecular structure of 1:1 Ru:**btp** complex [Ru(**15e**)Cl₂(DMSO)]. Co-crystallised molecule of unbound ligand **15e** has been omitted for clarity.¹¹¹; (c) Molecular structure of heteroleptic complex [Ru(**40a**)(4-Br- ϕ -**terpy**)](PF₆)₂. Solvent molecules and counterions have been omitted for clarity.⁹⁸

Cite this: DOI: 10.1039/c0xx00000x

www.rsc.org/xxxxxx

ARTICLE TYPE



Hecht and co-workers have also described the synthesis of coordinatively saturated complexes of the form [Ru(**btp**)₂](PF₆)₂ with ligands **15c**, **34**, **37** and **38**, as well as a heteroleptic system [Ru(**15c**)(**15d**)](PF₆)₂, prepared by treatment of [Ru(**15c**)Cl₂(DMSO)] with **15d** in the presence of NH₄PF₆. CV measurements of the four homoleptic complexes showed broadly similar behaviour. Qualitatively, however, the one-electron oxidation waves were strongly shifted depending on the attached ligand, particularly the electron-donating or -withdrawing properties of the substituent in the 4-pyridyl position of the **btp** ligand. The Ru(II) oxidation potential shifted over a range of more than 0.6 V with the range of ligands studied, from 0.58 V for **34**, with an electron-donating pyrrolidyl substituent to 1.19 V for **37** where the methyl ester substituent is electron-withdrawing. Variation of the 4-pyridyl substituents of these **btp** ligands was thus clearly shown to have a direct effect on the redox properties of the derived complexes, which is potentially predictable and tuneable. Furthermore, plotting the half-wave potentials of these complexes against the Hammett σ_{para} values of the substituents¹³² on the pyridyl moiety showed a clear linear relationship, further implying that predictable tuning of redox properties is possible by careful choice of ligand substituents. The effect of the ‘arms’ of the ligand (*i.e.* the *N*-triazolyl substituents) was observed to be minimal; with the complex of **15c** (which has a methyl terminal group in its ‘arms’) fitting the same linear relationship as all of the iodo-containing compounds.

Our research group has also shown the formation of monoleptic Ru(II) complex [Ru(**4a**)Cl₂(DMSO)], which displayed luminescence centred at 475 nm that was enhanced at 77 K.⁶¹ We also observed the same insensitivity to ‘arm’ substituents for our complexes [Ru(**4a-b**)₂](PF₆)₂, regardless of

whether the ‘arm’ was a methyl ester or carboxylic acid, the oxidation potentials were identical.⁶¹ This property theoretically allows for robust functionalisation of a product in this position after a desirable oxidation potential has been achieved, *e.g.* for multifunctional systems.

In recent years, Schubert and various co-workers have published prolifically in the field of Ru(II) coordination by **btp**-containing ligands, mostly with regard to the preparation of heteroleptic Ru(II)-complexes of **terpy** and **btp** ligands,^{97,98,100} and Ru(II) complexes containing π -conjugated ditopic **btp** ligands^{95,105,106}. A range of heteroleptic systems, [Ru(**39a-b**)(**terpy**)](PF₆)₂, [Ru(**39a-b**)(4-Br- ϕ -**terpy**)](PF₆)₂ and [Ru(**40a-b**)(4-Br- ϕ -**terpy**)](PF₆)₂ were prepared and studied, with homoleptic complexes [Ru(**39a**)₂](PF₆)₂ and [Ru(**terpy**)₂](PF₆)₂ used as reference systems with which properties were compared.

Single crystals suitable for X-ray diffraction studies were obtained of [Ru(**40a**)(4-Br- ϕ -**terpy**)](PF₆)₂, with the structure shown in Fig. 7(c). Compared to the homoleptic *bis*-**btp** complex, the interligand angle of the middle nitrogen atoms was shown to be closer to 180° (178.37° as opposed to 175°) and hence closer to the ideal undistorted octahedral geometry. The overall conclusion of this structural comparison was that the difference in coordination geometry when a **terpy** ligand is replaced with a **btp** ligand is only very small, hence from a coordination chemistry point of view, **btp** can be considered an analogue for **terpy** (*c.f.* discussion above).^{98,100}

The photophysical properties of the heteroleptic complexes were found to be between those of the reference homoleptic complexes. Complex [Ru(**39a**)(**terpy**)](PF₆)₂ displayed an intense MLCT band at a wavelength (432 nm) exactly half way between the MLCT bands shown by the two homoleptic complexes, while

the LC band was split in a distinctive fashion with two maxima corresponding to the peaks observed for the individual homoleptic complexes, indicating that the two ligands were electronically different in the Ru(II) coordination sphere. The blue-shift in the MLCT as **terpy** ligands were replaced with **btp** was attributed to more efficient back-bonding, raising the LUMO energy, as well as lowering of the HOMO with increasing π -acceptor character of the ligands.⁹⁸ It was also noted that whereas addition of the electron-withdrawing 4-bromophenyl group in the central 4-pyridyl position of **terpy** led to significant red-shift of the MLCT band, the variation of substituents between ligands **39**, **40** and **41** seemed to have negligible influence on the complexes' photophysical properties. This is in agreement with the insensitivity of electrochemical properties to 'arm' substituents described above.

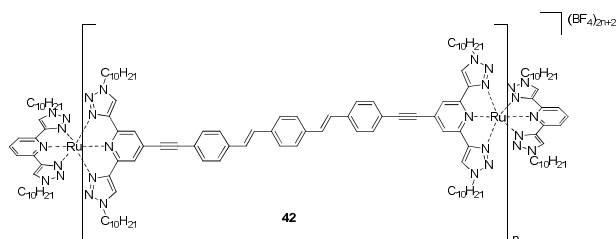


Fig. 8 Metallopolymer of **42**, capped with **39a**.

Ditopic ligands **17** and **42**, linked by π -conjugated spacers, were employed to form high-molar-mass Ru(II) coordination polymers.^{95,105,106} With the aim of producing printable polymers with interesting optoelectronic properties, long alkyl chain 'arms' were introduced in order to increase solubility and overcome π -stacking, which is a common disadvantage of conjugated systems. The structure of the Ru(II)-metallopolymer of **42** is shown in Fig. 8 as an example. The ligands were reported to have high extinction coefficients and medium to high quantum yields. With increased conjugation, the absorption became more intense and red shifted compared to 4-bromo substituted precursor ligand **16**, while the emission was slightly red shifted. Only the analogous polymer formed from **17** had any emission, albeit weak, assigned to the conjugated linker stabilising the **btp** ³MLCT state. These metallopolymer were measured as being less viscous than analogous **terpy** polymers, which was suggested to arise from the greater steric freedom of the **btp** motif displays over **terpy**, which Flood and co-workers have commented upon.⁵⁹ Microscopy measurements performed upon the polymers using both AFM and TEM imaging techniques, showed relatively rigid rod-like structures, which exhibited some aggregation and coiling, however smooth films could be formed on a quartz slide by drop-casting, indicating solution processability.

Compounds **43a–b** were designed as polymerisation precursors. Munuera and O'Reilly exploited the metal complexation ability of these **btp** motifs to introduce a coordination domain into the derived polymers so as to form higher order structures. In this case, utilizing the ability of Ru(II) to afford *bis*-chelated systems, 4-armed 'star' metallo-polymers were obtained after polymerisation.¹²⁹ Ru(II) has been used to template the geometry of 'star-branched polymers' by Kakuchi and co-workers as well. These will be discussed further in

Section 5.5.^{60,133}

2.11 Lanthanides

The Ln(III) ions have attracted significant attention because of their unique magnetic and photophysical properties,^{134–137} particularly their ability to provide long-lived characteristic and line-like emission upon sensitisation by coordinated ligands *via* the 'antenna effect' and consequently in their applications in supramolecular self-assembly chemistry, as our group has demonstrated in series of publications.^{16–19,53,58,138–141} Hence they lend themselves to use in other applications such as in biological sensing, OLEDs, and as imaging agents, *etc.*^{142,143}

Flood and co-workers proved that **btp**-ligand **3a** could form a stable coordination complex with Eu(III), which is to the best of our knowledge, the first example of such a system in the literature. X-Ray diffraction studies demonstrated that three terdentate ligands were required to satisfy the high coordination numbers of Eu(III) (the molecular structure of [Eu(**3a**)₃](ClO₄)₃ is shown in Fig. 9).⁵⁹ When compared with its **terpy** analogue, [Eu(**terpy**)₃](ClO₄)₃, subtle differences in the geometry were noted: whereas each pyridyl ring in the **terpy** ligand was seen to be tilted at angles to each other in order to avoid steric effects, the steric freedom afforded by the 1,2,3-triazole rings allowed the entire ligand to be almost planar and for each **3a** ligand to be mutually orthogonal. It was concluded, therefore, that the complex was more isotropic than its **terpy** analogue.¹⁴⁴ The complex exhibited characteristic line-like Eu(III) emission in solution, indicating coordination of **3a** to the metal centre and excitation of the ion by the 'antenna effect'.

Hecht and co-workers reported the synthesis of complexes [Eu(**15c**)₃](CF₃SO₃)₃ and [Eu(**15e**)₃](CF₃SO₃)₃. They also concluded from comparison of the X-ray crystal structure of [Eu(**15c**)₃](CF₃SO₃)₃ with **terpy** and also **bpp** analogues that the planar **btp** ligands are more favourable to the formation of Ln(III) complexes, providing better donor capabilities as well as increased steric freedom compared to the other terdentate azaaromatic ligands.⁷¹ These systems also display the characteristic red Eu(III) luminescence in both solid state and solution.

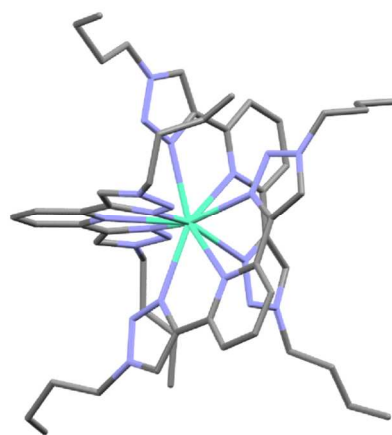


Fig. 9 Molecular structure of [Eu(**3a**)₃](ClO₄)₃. Hydrogens and counterions have been omitted for clarity.

The synthesis of π -conjugated fluorescent back-to-back ditopic

btp ligands was identified as a target by Chandrasekhar and Chandrasekar. These systems were ideal for coordination of Ln(III) ions because of the presence of the tridentate chelating motifs in both the front and back positions, allowing them to shield the ions completely from solvent molecules, thereby reducing solvent quenching of Ln(III) luminescence.¹⁰² Three ditopic ligands **9a–c** were prepared with up to two phenyl linkers between the two **btp** units (see Scheme 3). Only the self-assembly of **9b** with Eu(III) was studied. The complex exhibited Eu(III)-centred luminescence bands, arising from the ‘antenna effect’. The emission spectra are typical of complexes with low metal ion site symmetry, and are dominated by the hypersensitive $^5D_0 \rightarrow ^7F_2$ transition.

More recently, complexes of ligand **1** with Sm(III), Eu(III), Tb(III) and Dy(III) have been evaluated as chemically stable bioimaging agents, suggesting significant potential future applications of such systems in a medical context.¹⁴⁵

The **btp** motif has allowed exploitation of the Ln(III) coordination geometry and properties for applications with surfaces and materials. For instance, Brunet *et al.* described the covalent attachment of ligands **44** and **45** to a γ -zirconium phosphate surface, where they acted as sensitisers for Ln(III) emission and also circularly polarised luminescence (CPL) in the case of the chiral ligands.^{94,146} In a further example, compounds **43a–b** acted as agents for RAFT (reversible addition fragmentation chain transfer) polymerisation, producing polymers which could be templated by Eu(III) to form 6-arm ‘star-branched’ polymers.¹²⁹ These applications will be discussed in more detail in Section 5.2 below.

Weng and co-workers reported the synthesis of multi-responsive self-healing metallo-supramolecular gels made from **btp**-containing polymers **28** and **29** which coordinated Eu(III) and Tb(III). The Eu(III) emission from these gels was quenched by heating (upon reversible conversion to sols), making such materials potentially valuable as luminescent temperature sensors. These systems will be discussed in Section 5.6.^{117–119}

2.12 Other metal-containing systems

There are two other metal-containing **btp** systems that merit mentioning for completeness, although in, both cases, coordination of the metal ion was not through the terdentate motif itself, but rather through appended moieties.

Crowley and co-workers have reported the synthesis of ligand **6**, which had Fe(II)-containing organometallic ferrocenyl groups in its ‘arms’. This compound crystallised in the triclinic space group P-1 and showed the characteristic *anti-anti* conformation of an uncoordinated ligand with the cyclopentadienyl rings of the ferrocene units in an eclipsed conformation.⁹¹

Hecht and co-workers described the preparation of an interesting ligand **46**, which incorporated zinc porphyrin-appended ‘arms’; further work on this system has not been forthcoming.⁷¹

3. Interactions with anions

As well as interaction with metal ions, 1,2,3-triazoles have the ability to interact with anions *via* the triazolyl CH, and are capable of simultaneously binding metal ions and halide ions from salts,¹⁴⁷ or templating the formation of interlocked

structures.^{148,149} Considering this property of the triazoles, literature relating to the interactions between the **btp** motif and various anions is remarkably rare.⁸⁴

Flood’s group were the first to investigate the interactions between halide anions and **btp**-containing systems.⁸⁷ Following on from previous studies on tetraphenylene-based triazolophanes **47**, as shown in

Fig. 10,^{150,151} it was deemed of interest to introduce pyridyl rings in place of two of the phenyl rings in these systems to alter the electronic character and size of the binding sites. The resulting triazolophanes **18a** and **18b** (see Scheme 7) were designed with a view to destabilising the 1:1 complexes formed with the tetraphenylene-based triazolophanes in favour of a 2:1 ‘sandwich’ complex with the halide ions.

Halide binding of **18a** was studied using UV-vis titrations, with addition of F^- , Cl^- , and Br^- leading to an absorbance minimum at 0.5 equivalents, owing to the 2:1 ‘sandwich’ complex. Further addition of halide ions was shown to result in the formation of 1:1 complexes. The 2:1 complex with I^- was shown to be persistent in solution, in contrast to the other halides. A preliminary crystal structure (only partially solved as a result of weak diffraction) of $[18b_2 \cdot I]TBA$ was presented which suggested the formation of a 2:1 ‘sandwich’ complex with this ligand in the

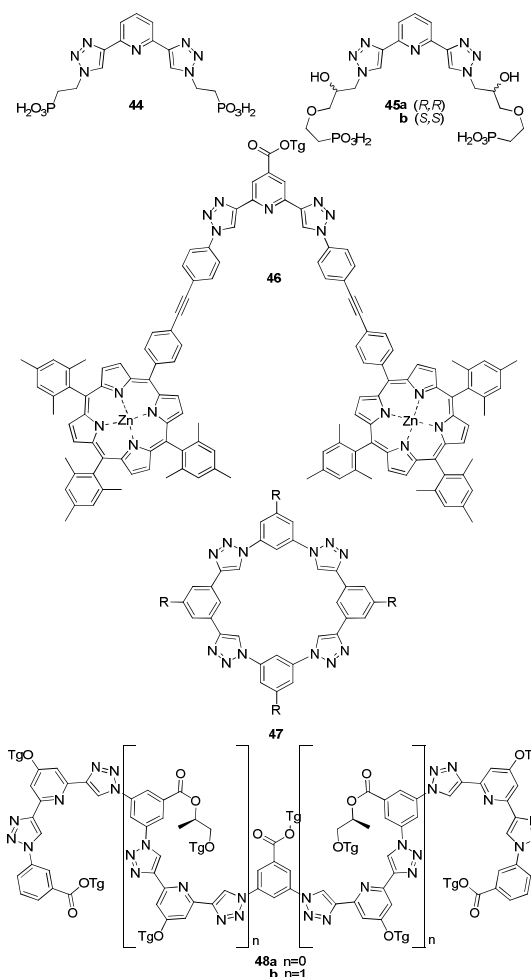


Fig. 10 Ligands **44** and **45**, porphyrin-containing system **46**, general structure of triazolophanes **47** and foldamers **48**.

solid state. This **btp**-containing triazolophane framework was also investigated as a potential ionophore with selectivity towards halides in ion-selective electrodes.¹⁵² Studies of the potentiometric responses of the **18a** based electrode towards various anions showed selectivity towards Γ^- .

The complex $[\text{Zn}(\mathbf{2})]^{2+}$, discussed above in Section 2.3, has a coordinatively unsaturated coordination sphere. The solvent molecules which occupy the three remaining positions could be readily displaced by anionic ligands and such behaviour should affect the emission of the system. The interactions of the complex with various anions were studied, with a view to its application as an anion chemosensor.^{107,108} Of a range of anions studied, including halides, thiocyanate, and nitrate, which were indeed shown to quench the complex's fluorescence upon addition in solution, the most remarkable results were observed for cyanide and nitrite ions.

Complexes of ligand **4a** and **4b** (Scheme 2) showed non-classical triazolyl C–H...Cl⁻ bonding in the solid state structures of $[\text{Ru}(\mathbf{4b})_2](\text{PF}_6)\text{Cl}$, $[\text{Ni}(\mathbf{4a})_2](\text{PF}_6)\text{Cl}$ and $[\text{Ir}(\mathbf{4a})\text{Cl}_3]$. The lengths and angles for these interactions were very similar across the series with H...Cl distances of 2.6–2.8 Å and with donor–acceptor distances being between 3.3–3.6 Å. The Cl⁻ was located approximately 134° out of the plane of the C–H bond in all cases.⁶¹

Hecht and co-workers described oligomeric systems **48** (see Fig. 10) which behaved as helically folding foldamers as a result of π – π stacking interactions.⁸⁸ As described in Section 1.3.8, oligomer **48b** was expected to undergo a structural change from *syn-syn* to *anti-anti* conformation upon protonation. Surprisingly, this effect was not observed upon addition of HCl as a source of protons, and in fact, the addition caused exact inversion of the circular dichroism (CD) signal of the helix, indicating an inversion of helicity; the inversion being proposed to arise from the presence of the Cl⁻ anion. Changes in the CD spectrum were also observed upon addition of F⁻ (increased intensity) and Br⁻ (inverted helicity and increased intensity). This is thought to be the first example of an achiral stimulus (halide ions) which promotes inversion of helicity in a foldamer.

4. Btp derivatives for photosensitiser and DSSC applications

In recent years, with photosensitiser applications in mind, a

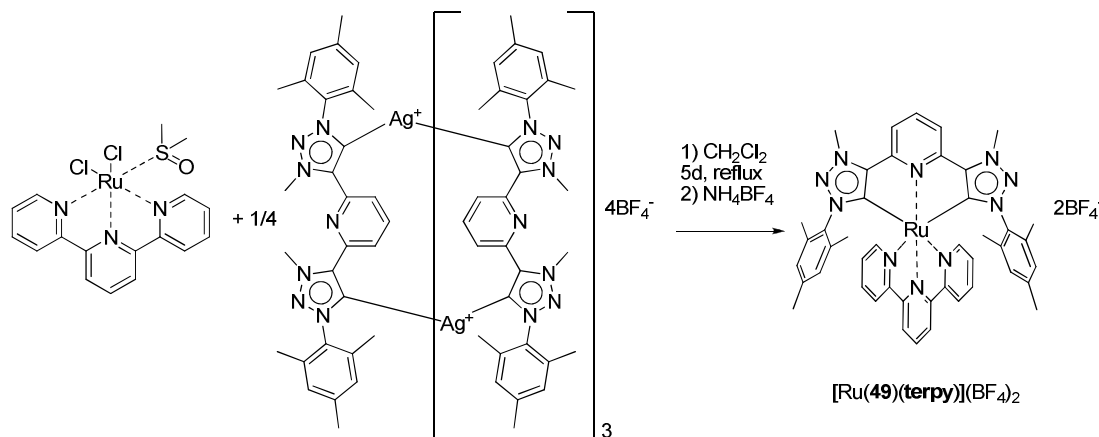
number of interesting systems, derived from **btp** have been reported. These will be briefly discussed.

The first such system reported by Schubert and co-workers was an *N*-heterocyclic carbene (NHC) **btp** triazolium derivative, **49**.⁹⁷ When compared to N[^]N[^]N[^] **btp** ligands, this C[^]N[^]C carbene ligand was proposed to have superior σ -donating and only moderate π -accepting properties, which would destabilise the ³MC state and maintain the energy of the ³MLCT state, leading to the desired reduction in radiationless deactivation and hence an increase in excited-state lifetime compared to the (generally non-luminescent) Ru(II)–**btp** complexes.

Cyclometallated complex $[\text{Ru}(\mathbf{49})(\text{terpy})](\text{BF}_4)_2$ was prepared, *via* a Ag(I)-carbene intermediate, Scheme 11, which prevented ligand **49** from undergoing a 5–3 methyl shift. The complex was shown by X-ray crystallography to display C[^]N[^]C-pincer coordination of the Ru(II) ion by the carbene ligand. The excited state lifetime measured (633 ns) is of similar magnitude to tris-bidentate $[\text{Ru}(\text{bipy})_3](\text{PF}_6)_2$ and 2500 times longer than the analogous bis(**terpy**) complex. The photophysical and electrochemical properties of this system are promising for photosensitiser applications.

Berlinguette and co-workers also studied ligand **49**, along with **50** and the phosphonate derivative **51** for the purposes of stabilising Ru(II) sensitisers' anchoring to TiO₂ semiconductor surfaces, an important consideration in applying photosensitisers to dye-sensitised solar cell (DSSC) applications. This is usually achieved by introduction of a carboxylate 'anchoring group' into the sensitiser to provide electronic coupling to the semiconductor. However, these bonds are susceptible to hydrolysis if any water is present in the system. It was thought phosphonates would provide a more robust linkage, but lower charge-injection rates.

Four photosensitisers were prepared, $[\text{Ru}(\mathbf{49})(\text{CO}_2\text{H-terpy})]^{2+}$, $[\text{Ru}(\mathbf{50})(\text{CO}_2\text{H-terpy})]^{2+}$, $[\text{Ru}(\mathbf{51})(\text{terpy})]^{2+}$ and $[\text{Ru}(\mathbf{51})(\text{CO}_2\text{H-terpy})]^{2+}$, with carboxylate and/or phosphonate 'anchoring groups'. The study showed that the distinctive properties of different 'anchoring groups' could be exploited with the carboxylate on the ligand responsible for electronic communication with the semiconductor surface and using the stronger-binding phosphonates to provide a robust linkage between ligand and surface. This was concluded to be a broadly applicable strategy.⁹²



Scheme 11 Synthesis of $[\text{Ru}(\mathbf{49})(\text{terpy})](\text{BF}_4)_2$.⁹⁷

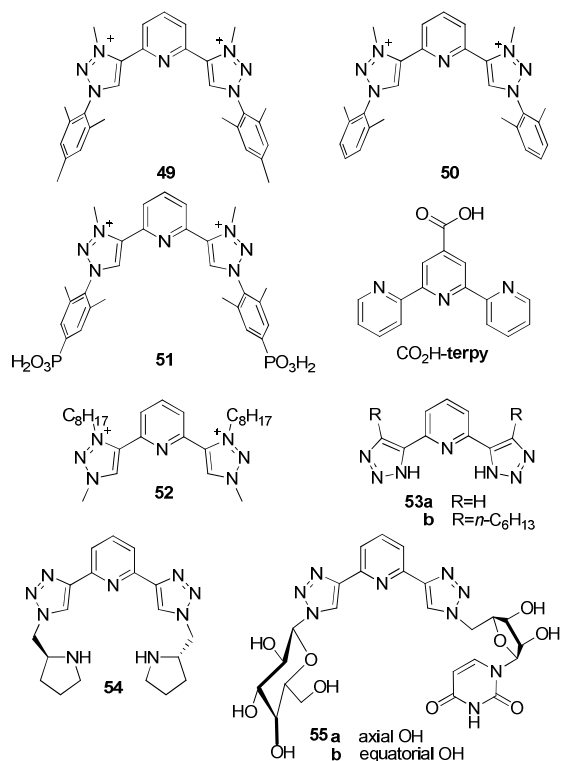
Cite this: DOI: 10.1039/c0xx00000x

www.rsc.org/xxxxxx

ARTICLE TYPE

More recently, ligand **52** has been prepared, with hydrophobic alkyl chains installed to increase solubility. Heteroleptic Ru(II) complexes with carboxylate-appended **terpy** of **52** only gave modest power conversions.¹⁵³

5 Anionic 1,2,3-triazolate derivatives of **btp** have also been reported, such as **53**. These ligands have increased σ - and π -donor strengths, shifting the MLCT of Ru(II) complexes to longer wavelengths. These systems also possessed photophysical and electrochemical properties appropriate to use in DSSCs, showing
10 promising performance with different types of electrolytes.¹⁵⁴



5. Further applications

Btp ligands have been employed in several applications other than those discussed above. We will now highlight these in
15 several subsections, demonstrating that the **btp** motif has an important future as a supramolecular framework.

5.1 Catalysis

A symmetrical **btp** ligand with chiral pyrrolidin-2-ylmethyl arms **54** was synthesised as part of a study into new organo-catalysts
20 for asymmetric Michael additions.⁹⁹ Compared with the other catalysts designed in the study (the **btb** analogue and a mono-(triazolyl)pyridyl analogue), **54** was the most diastereo- and enantioselective and, although slower than the other catalysts, the test reaction (Michael addition of cyclohexanone to nitrostyrene)
25 proceeded to completion without any additives. It also showed

activity for a range of substituted β -nitrostyrenes.

As briefly mentioned in Section 1.3 above, **1** was first synthesised as a ligand to stabilise Cu(I) catalyst in solution and increase the rate of the CuAAC reaction, although it was not the
35 most effective ligand studied for this purpose.⁸⁹

5.2 Enzyme inhibition

As part of a range of compounds designed as inhibitors of glycosyltransferase enzymes, asymmetric compounds **55**, containing both a nucleoside and a carbohydrate 'arm', were
35 synthesised and evaluated. The particular enzymes studied were metal-dependent galactosyltransferases, and it was shown that the inhibitors chelated the Mn(II) ion. **55a**(axial) was a potent inhibitor of β -1,4-GalT and a weak inhibitor of the other enzymes, while **55b** was a weaker inhibitor.¹⁵⁵

5.3 Molecular logic gates

The responses of molecular sensors to stimuli (temperature, pH or particular species such as metal ions) can be harnessed in the fabrication of molecular devices using Boolean logic with careful design, provided inputs and outputs can be clearly interpreted.
45 The creation of logic gates from fluorophores that can mimic electronic counterparts has been reported and discussed, particularly by de Silva and co-workers.¹⁵⁶⁻¹⁵⁸

A number of research groups have reported differing responses of **btp** ligands to various metal ions, particularly with respect to
50 enhancement or quenching of ligand emission. The groups of Abarca,^{107,108} Zhu¹¹⁵ and Dash¹¹⁶ have all reported significant fluorescence enhancements of various ligands (**2**, **23**, **24**, **25**, **5**, **26** and **27**) upon addition of Zn(II) to solutions of the ligands as discussed above. They have also all reported quenching of
55 fluorescence upon addition of other divalent metal ions, such as Fe(II), Cu(II) and Pb(II). Dash and co-workers were first, however, to bring these two responses together in the fabrication of a molecular logic gate, using heavy metal ions as inputs.

Table 1 Truth table for logic gate for detection of Zn(II) and Fe(II) by **27**
60 at pH 7.0.¹¹⁶

Input 1 Zn(II)	Input 2 Fe(II)	Output (25 μ M 27) Intensity _(390 nm)
0 (0 μ M)	0 (0 μ M)	0
1 (25 μ M)	0 (0 μ M)	1
0 (0 μ M)	1 (25 μ M)	0
1 (25 μ M)	1 (25 μ M)	1

Sensor **27** was found to bind Zn(II) selectively and provide 20-fold emission enhancement (a 'switch-on' response), whereas Fe(II) led to a significant 'switch-off' response. Usefully,
65 however, the sensor was much more selective (28-fold) for Zn(II) than Fe(II), and hence the emission was enhanced by Zn(II)-coordination, even in the presence of Fe(II), with quenching occurring only in the presence of Fe(II) alone.¹¹⁶ The change in fluorescence intensity of the system around 390 nm was taken as

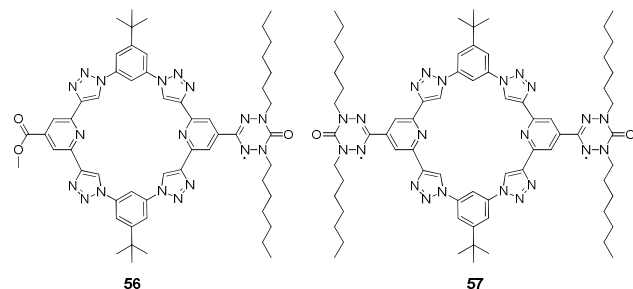
the output. The truth table drawn up for these changes is given in **Table 1**.

Here, the emission of **27** alone [input(0,0)] at 390 nm was very weak and is was assumed as 0 for the logic operation. The addition of one equivalent of Zn(II) led to the 20-fold increase in fluorescence intensity [input(1,0)] and is taken as a signal of 1 for the logic operation. In the presence of Fe(II) only [input(0,1)], the fluorescence intensity was quenched, giving a signal designated as 0, while the presence of 1 equivalent each of Zn(II) and Fe(II) [input(1,1)], the signal was enhanced, due to the high affinity of **27** for Zn(II) and this output was read as 1. The logic behaviour can be represented as a modified YES gate (with Fe(II) input left unconnected to the output). This is a remarkable and creative application of previously-observed properties of such **btp** systems.

5.4 Wave-guiding nanomaterials

Reversibly shape-shifting organic nanostructures which have waveguiding properties dependent on their dimensionality had never been reported before Chandrasekar and Chandrasekar produced such materials from the ditopic planar **btp** ligand **9b** (see Scheme 3).

The mechanical deformation mechanisms were studied and included use of sonication, solvent changes and time-dependent self-assembly, allowing interconversion between nanosheets, nanotubes and nanorings (*i.e.* two-, one- and zero-dimensional materials). The nanostructures were determined by various microscopy methods (including SEM, FESEM and TEM).¹¹⁰



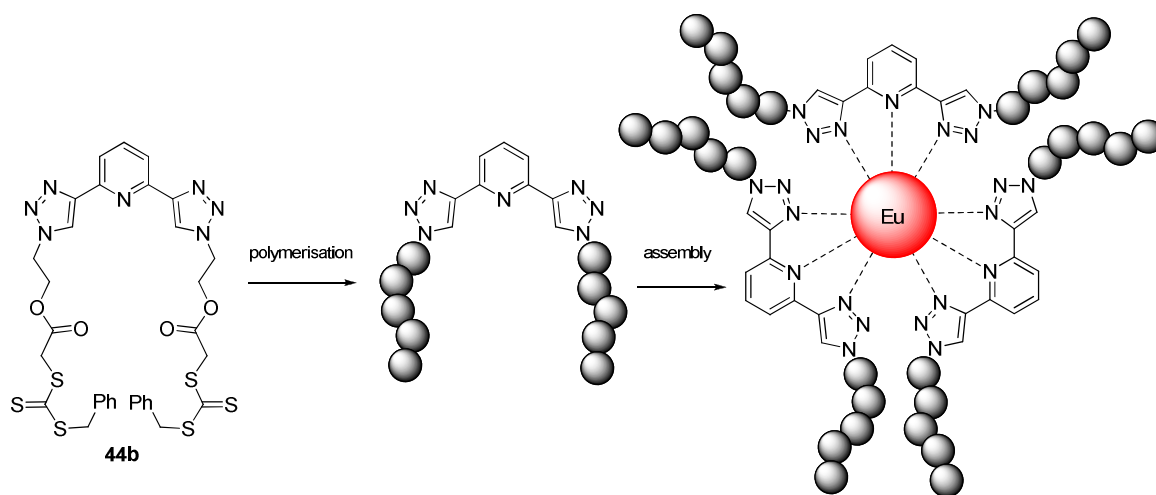
The optical waveguiding properties of these various nanostructures were studied by laser confocal microscopy. When an Ar laser beam output (488 nm) was focussed orthogonally on the centre of a 2D nanosheet, light was found to propagate in all four directions, while focussing light on one edge preferentially directed light mostly to the opposite edge. Focussing the laser beam on the centre of the 1D nanotubes led to light propagation from both open ends of the tube, while focussing the beam on one end resulted in light propagation out of the other end. This demonstrated that optical waveguiding behaviour in 1D or 2D was dependant on the nanostructures of **9b**, which could readily undergo shape-shifting between the 1D and 2D forms.¹¹⁰

The same group also reported paramagnetic hexagonal organic micro-tubes self-assembled from shape-persistent macrocycles **56** and **57**, which guided laser light from one end to the other.¹⁵⁹

5.5 Incorporation into polymers, macromolecules and surfaces

The use of CuAAC reactions to construct various polymers and dendrimers has been reviewed by Turro *et al.*⁷⁹ Only a limited number of compounds containing the **btp** motif have been used for these purposes.

By installing chelating functionalities into polymers *via* the ‘click-to-chelate’ approach (such as architectures **58**), Kakuchi and co-workers assembled 3- and 4-arm ‘star-branched’ polymer structures about a Ru(II) centre, using the metal centre to determine the assembly geometry.^{60,133} Study of an analogous complex [Ru(**1**)₂](PF₆)₂ confirmed the geometry of the polymer-appended complex. Polymers such as polystyrene, poly(*n*-butyl acrylate), poly(*n*-hexyl isocyanate), poly(caprolactone) and poly(styrene oxide) were used in various combinations. The polymer appended **btp** ligands **58** were prepared by the reaction of an azido-terminated polymer with 2,6-diethynylpyridine. Asymmetric ligands could also be prepared stepwise and complexes could be prepared as either homoleptic or heteroleptic star-branched polymers or copolymers. This proved a convenient methodology to introduce chelating sites into macromolecules, making them candidates for metal-templated synthesis.



Scheme 12 Illustration of the polymerisation–assembly strategy employed by Munuera and O’Reilly leading to formation of 6-arm ‘star-branched’ polymer templated by Eu(III).¹²⁹

Cite this: DOI: 10.1039/c0xx00000x

www.rsc.org/xxxxxx

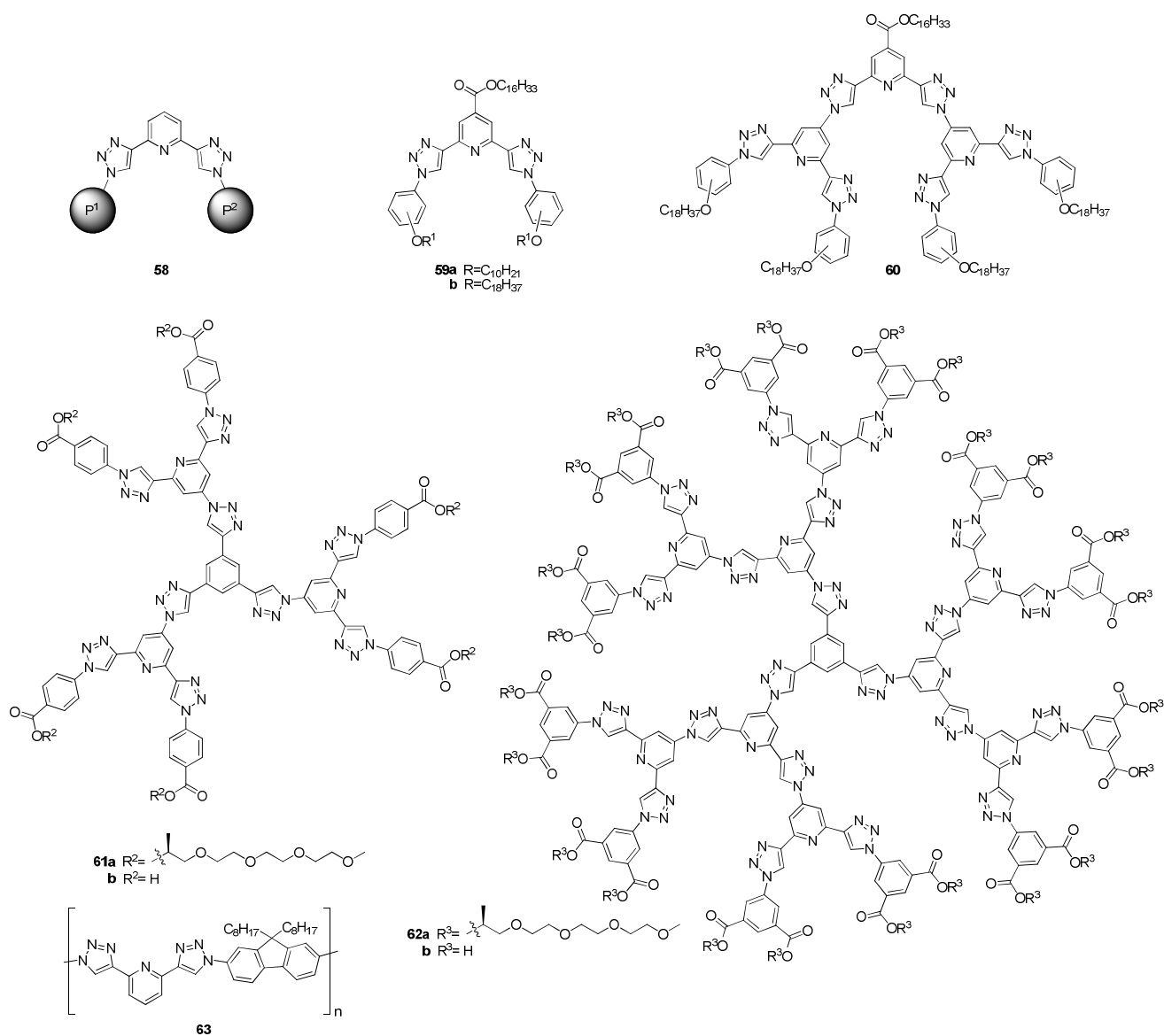
ARTICLE TYPE

Ligands **43a–b** were designed by Munuera and O'Reilly as RAFT polymerisation initiators containing the terdentate **btp** core. Polymerisation (e.g. with styrene or methyl methacrylate) followed by assembly around a Ru(II) or Eu(III) metal centre led to the formation of 4- or 6-arm 'star' polymers in the manner illustrated in Scheme 12.¹²⁹

Hecht and co-workers described the formation of first and second generation **btp** dendrons **59** and **60**, which were studied upon self-assembly at the solid-liquid interface upon physisorption on highly oriented pyrolytic graphite (HOPG).^{112,160} The three regioisomers of **59b** displayed ordered 2D self-assembly patterns in STM images, however, pronounced

effects upon the self-assembly of the monolayers were noted as a result of differing substitution patterns of the phenyl rings. Protonation of **59** upon addition of trifluoroacetic acid caused structural reorganisation to occur at the solid-liquid interface; the authors concluded this was as a result of interconversion from *anti-anti* ('kinked') to *syn-syn* ('extended') geometry. This reorganisation (from 'rosette' to 'tetragon' motifs) of the *meta*-isomer of **59b** was possible to observe in real-time over about 20 minutes.¹⁶⁰

Upon similar acidification of the *meta*-isomer of **60**, the conformation of the compound was also concluded to invert, with



25

Cite this: DOI: 10.1039/c0xx00000x

www.rsc.org/xxxxxx

ARTICLE TYPE

previous 'disordered' domains reorganizing into 'lamellar' assemblies.¹¹² Related shape-persistent flat dendrimers **61** and **62** behaved as disc-like amphiphiles, which stacked into cylindrical nanorods. The dendrimers with chiral tetra(ethyleneglycol) chains (viz. **61a** and **62a**) showed CD signals in aqueous solution, which was used to monitor the aggregation process. They also show thermo sensitive transition from nanorods to a 2D hexagonal columnar lattice.¹⁶¹

Polymer **63** was prepared *via* a CuAAC reaction, yielding a soluble material which was employed as a suitable support for metal loading with Pd(II), where ¹H NMR spectroscopy and elemental analysis were used as evidence of successful loading (the same research also yielded products with different spacers between the **btp** motifs, which were not further investigated).¹²³

Organic phosphonates can be covalently attached to the surface of the inorganic species γ -zirconium phosphate by topotactic exchange, and as such, a **btp**-based phosphonate ligand **44** was prepared, with a view to producing a solid host which could efficiently sensitise the emission of Ln(III) ions (Eu(III) and Tb(III), specifically) *via* the 'antenna effect'.⁹⁴

Compound **44** was also introduced into the inorganic framework by simply suspending the γ -zirconium phosphate colloiddally in a water-acetone mixture at 80 °C for a few minutes with the ligand. Upon suspending this material with the chloride salts of Eu(III) and Tb(III), the expected line-like Ln(III) luminescence was measured from the material, consistent with sensitisation of the metal ion by the remarkable organic-inorganic material. γ -Zirconium phosphate is intrinsically dissymmetric, however in racemic mixtures no bulk optical activity was observed.

It had previously been shown that intercalating with an optically pure molecule gave rise to optical rotation.¹⁶² With this in mind, chiral ligands **45** were introduced covalently into the framework to combine the ability to sensitise Tb(III) emission with optical activity to produce weak CPL signals in the solid state, a seldom-measured phenomenon.¹⁴⁶

5.6 Metallo-supramolecular gels

Hecht and co-workers described two different systems of poly-**btp** polymers **48**⁸⁸ and **21**¹⁰¹ in which the **btp** motif adopted the *anti-anti* conformation, giving rise to a helical conformation in the extended heteroaromatic strands. The interactions of **48** with anions is discussed in Section 3, above. **21**, on the other hand, showed the capacity to interact with metal ions, such as Zn(II), Fe(II) and Eu(III), to form metallo-supramolecular cross-linked gels upon characteristic inversion of conformation of the **btp** group (discussed above in Section 1.3.8).¹⁰¹

Weng and co-workers have also reported a number of **btp**-polymers **28**^{117,119} and **29**¹¹⁸ which form metallo-supramolecular gels upon coordination with Zn(II), Eu(III) and/or Tb(III) (*vide supra*) which were described as 'biomimetic' bulk materials. The rheological and optical properties of these gels were studied with various combinations of metal ions. Mechanical properties of the

bulk gels can be tuned by changing the stoichiometric ratios of the metals and choosing the metal-ligand system. For instance Zn(II) forms stronger less dynamic complexes with higher density of cross-linking due to its different coordination number.

These systems were shown to display remarkable self-healing properties when simply kept in a saturated toluene atmosphere. It proved possible to heal gels of different metal ion ratios together to form integrated gels that could be subjected to deformations such as bending and stretching without breaking at the joints. This is evidence of the dynamic nature of the self-healing of these metallo-supramolecular polymers.^{117,119} These materials underwent reversible gel-sol transitions upon heating and cooling and, in the case of Eu(III)-containing gels, emission was quenched upon heating, allowing the system to be considered temperature sensors. They also showed sensitivity to chemical stimuli, for instance nerve gas agent mimic triethyl phosphate. Bidentate **bipy** was found to deconstruct Zn(II)-gels only and not Ln(III)-gels.¹¹⁷ Both of these systems involved polymeric poly-**btp** components. More recently, Weng and co-workers have also reported self-healing **btp** systems with stress-sensing abilities,¹⁶³ and PEG-linked systems, which formed multiresponsive gels both in the presence and absence of Eu(III).¹⁶⁴

We reported [Ru-**4b**₂](PF₆)Cl, the first example of a metal complex gelator derived from discrete mono-**btp** components, the X-ray crystal structure of which suggests that it is able to induce solvent gelation by the formation of supramolecular polymer chains through hydrogen bond interactions between the carboxylic groups, ethanol solvent molecules and chloride anions. A viscous yellow soft material was formed which, when immobilised on a quartz slide, exhibited ligand-centred emission much like that seen for the complex in solution. Using both SEM and HIM imaging techniques revealed the fibrous nature of this material, with fibre widths in the range of 100 ± 25 nm.⁶¹

4. Conclusions

The above account has clearly demonstrated that the **btp** motif shows a versatile range of coordination and supramolecular chemistry across *d*- and *f*-block metals as well as interacting with anions. Its applicability to wide-ranging fields, convenience of preparation and ease of derivatisation are all advantageous. From its first appearance in the literature in 2004 to date, the rate of **btp**-compounds being published has accelerated and looks set to continue as current researchers branch out in their use of these compounds and as the wider chemical research community becomes aware of the motif.

The **btp** motif is in many ways analogous to the ubiquitous **terpy** motif and other terdentate chelating architectures, allowing for its introduction into systems to vary the properties or characteristics of species previously purely based on **terpy** chemistry. Hecht and co-workers' application of **btp** ligands to Ru(II) poly-azaaromatic electrochemistry is an example of this kind of work. As has been shown in this article, the **btp** motif has

predictable coordination chemistry, with the ligands and anion-complexes favouring an *anti-anti* ('kinked') geometry and metal complexes and protonated species favouring *syn-syn* ('extended') geometry, both with essentially planar **btp** units. The interconversion of these geometries has been exploited.

The coordination chemistry of **btp** ligands with Ni(II), Cu(II), Zn(II), Ag(I), Ir(III), Pt(II), Pd(II), Pb(II), Fe(II), Ru(II), Sm(III), Eu(III), Tb(III) and Dy(III) has been detailed, along with the properties and applications of these various complexes and coordination polymers. The interactions with anions have been described. The related triazolium derivatives have been discussed with respect to their potential as photosensitisers. Applications in catalysis, enzyme inhibition, molecular logic, wave-guiding nanomaterials, incorporation into polymers, surfaces and metallo-supramolecular gels have been discussed in more detail; and it is clear that more such supramolecular and nano-applications will appear in the near future. This class of chelating ligand is likely to become increasingly relevant in the coming years, particularly in supramolecular chemistry, solar cell research, magnetism, molecular logic and materials chemistry. We look forward to these exciting future developments; it is clear that the **btp** ligand has a major role to play across many areas of chemistry in the future.

Acknowledgements

The authors would like to acknowledge the Irish Research Council (IRC) Embark Initiative, IRCSET for postgraduate studentships (to JPB) and a postdoctoral fellowship (to JAK), Science Foundation Ireland (SFI) for 2010 PI Award, and TCD School of Chemistry for financial support. We would like to thank and dedicate this review to the many people and key players listed above; their work has wonderfully influenced our research in the past few years and will, without a doubt, continue to do so in the future.

Notes and references

^a School of Chemistry and Trinity Biomedical Sciences Institute, Trinity College, Pearse St, Dublin 2, Ireland. Fax: +353 1 716 2628; Tel: +353 1 896 3459; E-mail: byrnej26@tcd.ie, gunnlaut@tcd.ie

^b Chemistry, Faculty of Natural & Environmental Sciences, University of Southampton, Highfield, Southampton, SO17 1BJ, United Kingdom

† The **btp** motif has also been called by other names in the literature, such as '**tripy**' (by Professor Ulrich Schubert and co-workers) and '**bitapy**' (in work by Professor Toyoji Kakuchi and co-workers). The term 'clickate' has also been used by Professor Stefan Hecht and co-workers to describe such systems.

- P. A. Brayshaw, J.-C. G. Bünzli, P. Froidevaux, J. M. Harrowfield, Y. Kim and A. N. Sobolev, *Inorg. Chem.*, 1995, **34**, 2068-2076.
- F. Renaud, C. Piguet, G. Bernardinelli, J.-C. G. Bünzli and G. Hopfgartner, *J. Am. Chem. Soc.*, 1999, **121**, 9326-9342.
- C. Platas-Iglesias, C. Piguet, N. Andre and J.-C. G. Bünzli, *J. Chem. Soc., Dalton Trans.*, 2001, 3084-3091.
- N. Ouali, B. Bocquet, S. Rigault, P.-Y. Morgantini, J. Weber and C. Piguet, *Inorg. Chem.*, 2002, **41**, 1436-1445.
- J.-M. Senegas, G. Bernardinelli, D. Imbert, J.-C. G. Bünzli, P.-Y. Morgantini, J. Weber and C. Piguet, *Inorg. Chem.*, 2003, **42**, 4680-4695.

- A.-L. Gassner, C. I. Duhot, J.-C. G. Bünzli and A.-S. Chauvin, *Inorg. Chem.*, 2008, **47**, 7802-7812.
- A. Aebischer, F. Gumy and J.-C. G. Bünzli, *PCCP*, 2009, **11**, 1346-1353.
- A. S. Chauvin, F. Gumy, D. Imbert and J. C. G. Bünzli, *Spectrosc. Lett.*, 2004, **37**, 517-532.
- A.-S. Chauvin, F. Gumy, D. Imbert and J.-C. G. Bünzli, *Spectrosc. Lett.*, 2007, **40**, 193-193.
- S. Mistri, E. Zangrando and S. C. Manna, *Inorg. Chim. Acta*, 2013, **405**, 331-338.
- D. A. Leigh, P. J. Lusby, A. M. Z. Slawin and D. B. Walker, *Angew. Chem. Int. Ed.*, 2005, **44**, 4557-4564.
- A.-M. L. Fuller, D. A. Leigh, P. J. Lusby, A. M. Z. Slawin and D. B. Walker, *J. Am. Chem. Soc.*, 2005, **127**, 12612-12619.
- A.-M. L. Fuller, D. A. Leigh and P. J. Lusby, *Angew. Chem. Int. Ed.*, 2007, **46**, 5015-5019.
- M. R. Halvagar and W. B. Tolman, *Inorg. Chem.*, 2013, **52**, 8306-8308.
- S. Tanase, P. M. Gallego, R. de Gelder and W. T. Fu, *Inorg. Chim. Acta*, 2007, **360**, 102-108.
- J. P. Leonard, P. Jensen, T. McCabe, J. E. O'Brien, R. D. Peacock, P. E. Kruger and T. Gunnlaugsson, *J. Am. Chem. Soc.*, 2007, **129**, 10986-10987.
- C. Lincheneau, R. D. Peacock and T. Gunnlaugsson, *Chem. Asian J.*, 2010, **5**, 500-504.
- C. Lincheneau, C. Destribats, D. E. Barry, J. A. Kitchen, R. D. Peacock and T. Gunnlaugsson, *Dalton Trans.*, 2011, **40**, 12056-12059.
- J. A. Kitchen, D. E. Barry, L. Mercks, M. Albrecht, R. D. Peacock and T. Gunnlaugsson, *Angew. Chem. Int. Ed.*, 2012, **51**, 704-708.
- D. E. Barry, J. A. Kitchen, M. Albrecht, S. Faulkner and T. Gunnlaugsson, *Langmuir*, 2013, **29**, 11506-11515.
- C. Lincheneau, B. Jean-Denis and T. Gunnlaugsson, *Chem. Commun.*, 2014, **50**, 2857-2860.
- A. de Bettencourt-Dias, S. Viswanathan and A. Rollett, *J. Am. Chem. Soc.*, 2007, **129**, 15436-15437.
- K. Matsumoto, K. Suzuki, T. Tsukuda and T. Tsubomura, *Inorg. Chem.*, 2010, **49**, 4717-4719.
- A. de Bettencourt-Dias, P. S. Barber, S. Viswanathan, D. T. de Lill, A. Rollett, G. Ling and S. Altun, *Inorg. Chem.*, 2010, **49**, 8848-8861.
- G. Desimoni, G. Faita and P. Quadrelli, *Chem. Rev.*, 2003, **103**, 3119-3154.
- A. de Bettencourt-Dias, P. S. Barber and S. Bauer, *J. Am. Chem. Soc.*, 2012, **134**, 6987-6994.
- D. L. Jameson, J. K. Blaho, K. T. Kruger and K. A. Goldsby, *Inorg. Chem.*, 1989, **28**, 4312-4314.
- M. A. Halcrow, *Coord. Chem. Rev.*, 2005, **249**, 2880-2908.
- M. A. Halcrow, *New J. Chem.*, 2013, 10.1039/c3nj00835e.
- K. H. Sugiyarto, D. C. Craig, A. D. Rae and H. A. Goodwin, *Aust. J. Chem.*, 1993, **46**, 1269-1290.
- M. Duati, S. Fanni and J. G. Vos, *Inorg. Chem. Commun.*, 2000, **3**, 68-70.
- M. Duati, S. Tasca, F. C. Lynch, H. Bohlen, J. G. Vos, S. Stagni and M. D. Ward, *Inorg. Chem.*, 2003, **42**, 8377-8384.
- M. Mydlak, M. Mauro, F. Polo, M. Felicetti, J. Leonhardt, G. Diener, L. De Cola and C. A. Strassert, *Chem. Mater.*, 2011, **23**, 3659-3667.

34. K.-L. Wu, S.-T. Ho, C.-C. Chou, Y.-C. Chang, H.-A. Pan, Y. Chi and P.-T. Chou, *Angew. Chem. Int. Ed.*, 2012, **51**, 5642-5646.
35. M. G. B. Drew, M. J. Hudson, P. B. Iveson, C. Madic and M. L. Russell, *J. Chem. Soc., Dalton Trans.*, 1999, 2433-2440.
36. S. V. Chapyshev, *Chemistry of Heterocyclic Compounds*, 2001, **37**, 861-866.
37. S. V. Chapyshev, *Mendeleev Commun.*, 1999, **9**, 164-165.
38. S. V. Chapyshev, R. Walton and P. M. Lahti, *Mendeleev Commun.*, 2000, **10**, 138-139.
39. T. G. Ostapowicz, M. Hölscher and W. Leitner, *Chem. Eur. J.*, 2011, **17**, 10329-10338.
40. T. Merckx, P. Verwilt and W. Dehaen, *Tetrahedron Lett.*, 2013, **54**, 4237-4240.
41. A. Fleming, J. Gaire, F. Kelleher, J. McGinley and V. McKee, *Tetrahedron*, 2011, **67**, 3260-3266.
42. J. Gaire, J. McGinley, A. Fleming and F. Kelleher, *Tetrahedron*, 2012, **68**, 5935-5941.
43. N. Wartenberg, O. Raccurt, E. Bourgeat-Lami, D. Imbert and M. Mazzanti, *Chem. Eur. J.*, 2013, **19**, 3477-3482.
44. E. S. Andreiadis, D. Imbert, J. Pecaut, R. Demadrille and M. Mazzanti, *Dalton Trans.*, 2012, **41**, 1268-1277.
45. J. G. Vos and J. M. Kelly, *Dalton Trans.*, 2006, 4869-4883.
46. J. P. Sauvage, J. P. Collin, J. C. Chambron, S. Guillerez, C. Coudret, V. Balzani, F. Barigelletti, L. De Cola and L. Flamigni, *Chem. Rev.*, 1994, **94**, 993-1019.
47. P. R. Andres and U. S. Schubert, *Adv. Mater.*, 2004, **16**, 1043-1068.
48. T. Kinoshita, J. T. Dy, S. Uchida, T. Kubo and H. Segawa, *Nature Photonics*, 2013, **7**, 535-539.
49. R. Sakamoto, S. Katagiri, H. Maeda and H. Nishihara, *Coord. Chem. Rev.*, 2013, **257**, 1493-1506.
50. T. Gunnlaugsson, S. Banerjee, J. A. Kitchen, S. Bright, J. E. O'Brien, D. C. Williams and J. M. Kelly, *Chem. Commun.*, 2013.
51. M. J. Hannon, P. S. Green, D. M. Fisher, P. J. Derrick, J. L. Beck, S. J. Watt, S. F. Ralph, M. M. Sheil, P. R. Barker, N. W. Alcock, R. J. Price, K. J. Sanders, R. Pither, J. Davis and A. Rodger, *Chem. Eur. J.*, 2006, **12**, 8000-8013.
52. F. S. Han, M. Higuchi, T. Ikeda, Y. Negishi, T. Tsukuda and D. G. Kurth, *J. Mater. Chem.*, 2008, **18**, 4555-4560.
53. O. Kotova, R. Daly, C. M. G. dos Santos, M. Boese, P. E. Kruger, J. J. Boland and T. Gunnlaugsson, *Angew. Chem. Int. Ed.*, 2012, **51**, 7208-7212.
54. J. A. Kitchen, E. M. Boyle and T. Gunnlaugsson, *Inorg. Chim. Acta*, 2012, **381**, 236-242.
55. P. Wang, Z. Li, G.-C. Lv, H.-P. Zhou, C. Hou, W.-Y. Sun and Y.-P. Tian, *Inorg. Chem. Commun.*, 2012, **18**, 87-91.
56. A. M. Nonat, A. J. Harte, K. Senechal-David, J. P. Leonard and T. Gunnlaugsson, *Dalton Trans.*, 2009, 4703-4711.
57. J. Dinda, S. Liatard, J. Chauvin, D. Jouvenot and F. Loiseau, *Dalton Trans.*, 2011, **40**, 3683-3688.
58. A. M. Nonat, S. J. Quinn and T. Gunnlaugsson, *Inorg. Chem.*, 2009, **48**, 4646-4648.
59. Y. Li, J. C. Huffman and A. H. Flood, *Chem. Commun.*, 2007, 2692-2694.
60. C. Zhang, X. Shen, R. Sakai, M. Gottschaldt, U. S. Schubert, S. Hirohara, M. Tanihara, S. Yano, M. Obata, N. Xiao, T. Satoh and T. Kakuchi, *J. Polym. Sci., Part A: Polym. Chem.*, 2011, **49**, 746-753.
61. J. P. Byrne, J. A. Kitchen, O. Kotova, V. Leigh, A. Bell, J. J. Boland, M. Albrecht and T. Gunnlaugsson, *Dalton Trans.*, 2014, **43**, 196-209.
62. K. Lashgari, M. Kritikos, R. Norrestam and T. Norrby, *Acta Crystallogr. Sect. C*, 1999, **55**, 64-67.
63. B. Schulze and U. S. Schubert, *Chem. Soc. Rev.*, 2014, 10.1039/c3cs60386e.
64. H. Struthers, T. L. Mindt and R. Schibli, *Dalton Trans.*, 2010, **39**, 675-696.
65. H. C. Kolb, M. G. Finn and K. B. Sharpless, *Angew. Chem. Int. Ed.*, 2001, **40**, 2004-2021.
66. V. V. Rostovtsev, L. G. Green, V. V. Fokin and K. B. Sharpless, *Angew. Chem. Int. Ed.*, 2002, **41**, 2596-2599.
67. R. Huisgen, in *1,3-Dipolar Cycloaddition Chemistry*, ed. A. Padwa, Wiley, New York, 1984, pp. 1-176.
68. A. Michael, *Journal für Praktische Chemie*, 1893, **48**, 94-95.
69. C. W. Tornøe, C. Christensen and M. Meldal, *J. Org. Chem.*, 2002, **67**, 3057-3064.
70. J. D. Crowley and P. H. Bandeen, *Dalton Trans.*, 2010, **39**, 612-623.
71. R. M. Meudtner, M. Ostermeier, R. Goddard, C. Limberg and S. Hecht, *Chem. Eur. J.*, 2007, **13**, 9834-9840.
72. M. G. Finn and V. V. Fokin, *Chem. Soc. Rev.*, 2010, **39**, 1231-1232.
73. M. Tropicano, N. L. Kilah, M. Morten, H. Rahman, J. J. Davis, P. D. Beer and S. Faulkner, *J. Am. Chem. Soc.*, 2011, **133**, 11847-11849.
74. M. Milne, K. Chicas, A. Li, R. Bartha and R. H. E. Hudson, *Org. Biomol. Chem.*, 2012, **10**, 287-292.
75. J. K. Molloy, O. Kotova, R. D. Peacock and T. Gunnlaugsson, *Org. Biomol. Chem.*, 2012, **10**, 314-322.
76. M.-L. Teysnot, L. Nauton, J.-L. Canet, F. Cisnetti, A. Chevy and A. Gautier, *Eur. J. Org. Chem.*, 2010, **2010**, 3507-03515.
77. Z. E. A. Chamas, X. Guo, J.-L. Canet, A. Gautier, D. Boyer and R. Mahiou, *Dalton Trans.*, 2010, **39**, 7091-7087.
78. X. Guo, J.-L. Canet, D. Boyer, A. Gautier and R. Mahiou, *J. Mater. Chem.*, 2012, **22**, 6117-6122.
79. J. A. Johnson, M. G. Finn, J. T. Koberstein and N. J. Turro, *Macromol. Rapid Commun.*, 2008, **29**, 1052-1072.
80. J. M. Holub and K. Kirshenbaum, *Chem. Soc. Rev.*, 2010, **39**, 1325-1337.
81. K. D. Hanni and D. A. Leigh, *Chem. Soc. Rev.*, 2010, **39**, 1240-1251.
82. T. L. Mindt, H. Struthers, L. Brans, T. Anguelov, C. Schweinsberg, V. Maes, D. Tourwé and R. Schibli, *J. Am. Chem. Soc.*, 2006, **128**, 15096-15097.
83. V. D. Bock, H. Hiemstra and J. H. van Maarseveen, *Eur. J. Org. Chem.*, 2006, **2006**, 51-68.
84. Y. Hua and A. H. Flood, *Chem. Soc. Rev.*, 2010, **39**, 1262-1271.
85. D. Schweinfurth, N. Deibel, F. Weisser and B. Sarkar, *Nachrichten aus der Chemie*, 2011, **59**, 937-941.
86. J. D. Crowley and D. A. McMoran, in *Click Triazoles*, ed. J. Košmrlj, Springer Berlin Heidelberg, 2012, vol. 28, pp. 31-83.
87. Y. Li, M. Pink, J. A. Karty and A. H. Flood, *J. Am. Chem. Soc.*, 2008, **130**, 17293-17295.
88. R. M. Meudtner and S. Hecht, *Angew. Chem. Int. Ed.*, 2008, **47**, 4926-4930.
89. T. R. Chan, R. Hilgraf, K. B. Sharpless and V. V. Fokin, *Org. Lett.*, 2004, **6**, 2853-2855.
90. B. Abarca, R. Ballesteros and M. Chadlaoui, *Tetrahedron*, 2004, **60**, 5785-5792.

91. J. D. Crowley, P. H. Bandeen and L. R. Hanton, *Polyhedron*, 2010, **29**, 70-83.
92. D. G. Brown, P. A. Schauer, J. Borau-Garcia, B. R. Fancy and C. P. Berlinguette, *J. Am. Chem. Soc.*, 2013, **135**, 1692-1695.
93. J. T. Fletcher, B. J. Bumgarner, N. D. Engels and D. A. Skoglund, *Organomet.*, 2008, **27**, 5430-5433.
94. E. Brunet, O. Juanes, L. Jiménez and J. C. Rodríguez-Ubis, *Tetrahedron Lett.*, 2009, **50**, 5361-5363.
95. B. Schulze, C. Friebe, S. Hoepfener, G. M. Pavlov, A. Winter, M. D. Hager and U. S. Schubert, *Macromol. Rapid Commun.*, 2012, **33**, 597-602.
96. P. Danielraj, B. Varghese and S. Sankararaman, *Acta Crystallogr. Sect. C*, 2010, **66**, m366-m370.
97. B. Schulze, D. Escudero, C. Friebe, R. Siebert, H. Görls, U. Köhn, E. Altuntas, A. Baumgaertel, M. D. Hager, A. Winter, B. Dietzek, J. Popp, L. González and U. S. Schubert, *Chem. Eur. J.*, 2011, **17**, 5494-5498.
98. B. Schulze, C. Friebe, M. D. Hager, A. Winter, R. Hoogenboom, H. Görls and U. S. Schubert, *Dalton Trans.*, 2009, 787-794.
99. T. Karthikeyan and S. Sankararaman, *Tetrahedron: Asymmetry*, 2008, **19**, 2741-2745.
100. B. Schulze, C. Friebe, M. D. Hager, A. Winter, R. Hoogenboom, H. Görls and U. S. Schubert, *Polym. Prepr.*, 2009, **50**, 252.
101. R. M. Meudtner and S. Hecht, *Macromol. Rapid Commun.*, 2008, **29**, 347-351.
102. N. Chandrasekhar and R. Chandrasekar, *J. Org. Chem.*, 2010, **75**, 4852-4855.
103. C. M. Amb and S. C. Rasmussen, *J. Org. Chem.*, 2006, **71**, 4696-4699.
104. M. Nettekoven and C. Jenny, *Organic Process Research & Development*, 2002, **7**, 38-43.
105. B. Schulze, C. Friebe, M. D. Hager, A. Winter and U. S. Schubert, *Polym. Prepr.*, 2009, **50**, 576.
106. B. Schulze, C. Friebe, S. Hoepfener, G. M. Pavlov, M. D. Hager, A. Winter and U. S. Schubert, *Polym. Prepr.*, 2011, **52**, 917-918.
107. R. Ballesteros-Garrido, B. Abarca, R. Ballesteros, C. Ramirez de Arellano, F. R. Leroux, F. Colobert and E. Garcia-Espana, *New J. Chem.*, 2009, **33**, 2102-2106.
108. R. Ballesteros-Garrido, E. Delgado-Pinar, B. Abarca, R. Ballesteros, F. R. Leroux, F. Colobert, R. J. Zaragoza and E. Garcia-Espana, *Tetrahedron*, 2012, **68**, 3701-3707.
109. D. Zornik, R. M. Meudtner, T. El Malah, C. M. Thiele and S. Hecht, *Chem. Eur. J.*, 2011, **17**, 1473-1484.
110. N. Chandrasekhar and R. Chandrasekar, *Angew. Chem. Int. Ed.*, 2012, **51**, 3556-3561.
111. M. Ostermeier, M.-A. Berlin, R. M. Meudtner, S. Demeshko, F. Meyer, C. Limberg and S. Hecht, *Chem. Eur. J.*, 2010, **16**, 10202-10213.
112. T. El Malah, A. Ciesielski, L. Piot, S. I. Troyanov, U. Mueller, S. Weidner, P. Samori and S. Hecht, *Nanoscale*, 2012, **4**, 467-472.
113. W. Henke, S. Kremer and D. Reinen, *Inorg. Chem.*, 1983, **22**, 2858-2863.
114. C. Ramirez de Arellano, E. Escriva, C. J. Gomez-Garcia, G. Minguez Espallargas, R. Ballesteros and B. Abarca, *CrystEngComm*, 2013, **15**, 1836-1839.
115. A. H. Younes, R. J. Clark and L. Zhu, *Supramol. Chem.*, 2012, **24**, 696-706.
116. G. C. Midya, S. Paladhi, S. Bhowmik, S. Saha and J. Dash, *Org. Biomol. Chem.*, 2013, **11**, 3057-3063.
117. J. Yuan, X. Fang, L. Zhang, G. Hong, Y. Lin, Q. Zheng, Y. Xu, Y. Ruan, W. Weng, H. Xia and G. Chen, *J. Mater. Chem.*, 2012, **22**, 11515-11522.
118. B. Yang, H. Zhang, H. Peng, Y. Xu, B. Wu, W. Weng and L. Li, *Polymer Chemistry*, 2014, **5**, 1945-1953.
119. J. Yuan, H. Zhang, G. Hong, Y. Chen, G. Chen, Y. Xu and W. Weng, *J. Mater. Chem. B*, 2013, **1**, 4809-4818.
120. M. Dobroschke, Y. Geldmacher, I. Ott, M. Harlos, L. Kater, L. Wagner, R. Gust, W. S. Sheldrick and A. Prokop, *ChemMedChem*, 2009, **4**, 177-187.
121. J. A. Bailey, M. G. Hill, R. E. Marsh, V. M. Miskowski, W. P. Schaefer and H. B. Gray, *Inorg. Chem.*, 1995, **34**, 4591-4599.
122. Y. Li, L. Zhao, A. Y.-Y. Tam, K. M.-C. Wong, L. Wu and Y. W.-W. Yam, *Chem. Eur. J.*, 2013, **19**, 14496-14505.
123. C. Lang, K. Pahnke, C. Kiefer, A. S. Goldmann, P. W. Roesky and C. Barner-Kowollik, *Polymer Chemistry*, 2013, **4**, 5456-5462.
124. J. A. Kitchen, J. Olguín, R. Kulmaczewski, N. G. White, V. A. Milway, G. N. L. Jameson, J. L. Tallon and S. Brooker, *Inorg. Chem.*, 2013, **52**, 11185-11199.
125. A. Noble, J. Olguín, R. Clérac and S. Brooker, *Inorg. Chem.*, 2010, **49**, 4560-4569.
126. J. Olguín and S. Brooker, *Coord. Chem. Rev.*, 2011, **255**, 203-240.
127. M. A. Halcrow, *Coord. Chem. Rev.*, 2009, **253**, 2493-2514.
128. B. Schulze, D. Escudero, C. Friebe, R. Siebert, H. Görls, S. Sinn, M. Thomas, S. Mai, J. Popp, B. Dietzek, L. González and U. S. Schubert, *Chem. Eur. J.*, 2012, **18**, 4010-4025.
129. L. Munuera and R. K. O'Reilly, *Dalton Trans.*, 2010, **39**, 388-391.
130. J.-P. Collin, S. Guillerez and J.-P. Sauvage, *J. Chem. Soc., Chem. Commun.*, 1989, 10.1039/c39890000776, 776-778.
131. R. P. Thummel, V. Hegde and Y. Jahng, *Inorg. Chem.*, 1989, **28**, 3264-3267.
132. L. P. Hammett, *J. Am. Chem. Soc.*, 1937, **59**, 96-103.
133. N. Xiao, Y. Chen, X. Shen, C. Zhang, S. Yano, M. Gottschaldt, U. S. Schubert, T. Kakuchi and T. Satoh, *Polym J*, 2013, **45**, 216-225.
134. J.-C. G. Bünzli, *Acc. Chem. Res.*, 2005, **39**, 53-61.
135. J.-C. G. Bünzli and C. Pigué, *Chem. Soc. Rev.*, 2005, **34**, 1048-1077.
136. C. M. G. dos Santos, A. J. Harte, S. J. Quinn and T. Gunnlaugsson, *Coord. Chem. Rev.*, 2008, **252**, 2512-2527.
137. J. P. Leonard, C. B. Nolan, F. Stomeo and T. Gunnlaugsson, *Top. Curr. Chem.*, 2007, **281**, 1-43.
138. O. Kotova, J. A. Kitchen, C. Lincheneau, R. D. Peacock and T. Gunnlaugsson, *Chem. Eur. J.*, 2013, **19**, 16181-16186.
139. C. Lincheneau, J. P. Leonard, T. McCabe and T. Gunnlaugsson, *Chem. Commun.*, 2011, **47**, 7119-7121.
140. F. Stomeo, C. Lincheneau, J. P. Leonard, J. E. O'Brien, R. D. Peacock, C. P. McCoy and T. Gunnlaugsson, *J. Am. Chem. Soc.*, 2009, **131**, 9636-9637.
141. S. Comby, F. Stomeo, C. P. McCoy and T. Gunnlaugsson, *Helv. Chim. Acta*, 2009, **92**, 2461-2473.
142. B. McMahon, P. Mauer, C. P. McCoy, T. C. Lee and T. Gunnlaugsson, *J. Am. Chem. Soc.*, 2009, **131**, 17542-17543.

143. B. K. McMahon, P. Mauer, C. P. McCoy, T. C. Lee and T. Gunnlaugsson, *Aust. J. Chem.*, 2011, **64**, 600-603.
144. G. H. Frost, F. A. Hart, C. Heath and M. B. Hursthouse, *J. Chem. Soc. D, Chem. Commun.*, 1969, 10.1039/c29690001421, 1421-1422.
- 5 145. A. Indapurkar, B. Henriksen, J. Tolman and J. Fletcher, *J. Pharm. Sci.*, 2013, **102**, 2589-2598.
146. E. Brunet, L. Jiménez, M. de Victoria-Rodríguez, V. Luu, G. Muller, O. Juanes and J. C. Rodríguez-Ubis, *Microporous Mesoporous Mater.*, 2013, **169**, 222-234.
- 10 147. S. C. Picot, B. R. Mullaney and P. D. Beer, *Chem. Eur. J.*, 2012, **18**, 6230-6237.
148. N. G. White and P. D. Beer, *Chem. Commun.*, 2012, **48**, 8499-8501.
149. M. S. Vickers and P. D. Beer, *Chem. Soc. Rev.*, 2007, **36**, 211-225.
150. Y. Li and A. H. Flood, *Angew. Chem. Int. Ed.*, 2008, **47**, 2649-2652.
- 15 151. Y. Li and A. H. Flood, *J. Am. Chem. Soc.*, 2008, **130**, 12111-12122.
152. E. M. Zahran, Y. Hua, S. Lee, A. H. Flood and L. G. Bachas, *Anal. Chem.*, 2011, **83**, 3455-3461.
153. S. Sinn, B. Schulze, C. Friebe, D. G. Brown, M. Jäger, E. Altuntaş, J. Kübel, O. Guntner, C. P. Berlinguette, B. Dietzek and U. S. Schubert, 20 *Inorg. Chem.*, 2014, **53**, 2083-2095.
154. S. Sinn, B. Schulze, C. Friebe, D. G. Brown, M. Jäger, J. Kübel, B. Dietzek, C. P. Berlinguette and U. S. Schubert, *Inorg. Chem.*, 2014, **53**, 1637-1645.
155. S. Wang, J. A. Cuesta-Seijo, D. Lafont, M. M. Palcic and S. Vidal, 25 *Chem. Eur. J.*, 2013, **19**, 15346-15357.
156. A. P. de Silva, H. Q. N. Gunaratne and C. P. McCoy, *Nature*, 1993, **364**, 42-44.
157. A. P. de Silva, H. Q. N. Gunaratne, T. Gunnlaugsson, A. J. M. Huxley, C. P. McCoy, J. T. Rademacher and T. E. Rice, *Chem. Rev.*, 30 1997, **97**, 1515-1566.
158. A. P. de Silva, *Molecular Logic-based Computation*, The Royal Society of Chemistry, Cambridge, 2012.
159. P. Hui and R. Chandrasekar, *Adv. Mater.*, 2013, **25**, 2963-2967.
160. L. Piot, R. M. Meudtner, T. El Malah, S. Hecht and P. Samori, *Chem. Eur. J.*, 2009, **15**, 4788-4792.
- 35 161. T. El Malah, S. Rolf, S. M. Weidner, A. F. Thünemann and S. Hecht, *Chem. Eur. J.*, 2012, **18**, 5837-5842.
162. E. Brunet, H. M. H. Alhendawi, O. Juanes, L. Jimenez and J. C. Rodríguez-Ubis, *J. Mater. Chem.*, 2009, **19**, 2494-2502.
- 40 163. G. Hong, H. Zhang, Y. Lin, Y. Chen, Y. Xu, W. Weng and H. Xia, *Macromolecules*, 2013, **46**, 8649-8656.
164. W. Weng, X. Fang, H. Zhang, H. Peng, Y. Lin and Y. Chen, *Eur. Polym. J.*, 2013, **49**, 4062-4071.

45